Vulnerability versus resilience to prenatal stress in male and female rats; Implications from gene expression profiles in the hippocampus and frontal cortex

ARTICLE *in* EUROPEAN NEUROPSYCHOPHARMACOLOGY: THE JOURNAL OF THE EUROPEAN COLLEGE OF NEUROPSYCHOPHARMACOLOGY · NOVEMBER 2012

Impact Factor: 4.37 · DOI: 10.1016/j.euroneuro.2012.09.011 · Source: PubMed

10 AUTHORS, INCLUDING:

Daniel Louis Albert Van den Hove
Maastricht University, University of Wuerzb…
89 PUBLICATIONS **1,615** CITATIONS
SEE PROFILE

Bart P F Rutten
Maastricht University
93 PUBLICATIONS **2,870** CITATIONS
SEE PROFILE

Matteo Bruschettini
Lund University
55 PUBLICATIONS **810** CITATIONS
SEE PROFILE

Harry W M Steinbusch
School for Mental Health and Neuroscience…
557 PUBLICATIONS **20,582** CITATIONS
SEE PROFILE

European Neuropsychopharmacology (2013) 23, 1226–1246

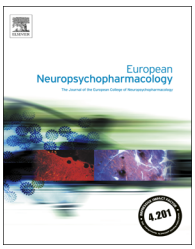

www.elsevier.com/locate/euroneuro

Vulnerability versus resilience to prenatal stress in male and female rats; Implications from gene expression profiles in the hippocampus and frontal cortex

D.L.A. Van den Hove[a,b,*,1], G. Kenis[c,1], A. Brass[d], R. Opstelten[a], B.P.F. Rutten[c], M. Bruschettini[a], C.E. Blanco[e], K.P. Lesch[a,b], H.W.M. Steinbusch[a], J. Prickaerts[a]

[a]*Department of Neuroscience, School for Mental Health and Neuroscience (MHeNS), Maastricht University, European Graduate School of Neuroscience (EURON), Universiteitssingel 50, P.O. Box 616, 6200 MD, Maastricht, The Netherlands*
[b]*Molecular Psychiatry, Department of Psychiatry, Psychosomatics and Psychotherapy, University of Wuerzburg, Fuechsleinstrasse 15, 97080 Wuerzburg, Germany*
[c]*Department of Psychiatry and Neuropsychology, School for Mental Health and Neuroscience (MHeNS), Maastricht University, European Graduate School of Neuroscience (EURON), Dr. Tanslaan 10, P.O. Box 616, 6200 MD Maastricht, The Netherlands*
[d]*Department of Computer Science, University of Manchester, Manchester M13 9PL, United Kingdom*
[e]*Department of Pediatrics, Research Institute Growth and Development (GROW), Faculty of Health, Medicine and Life Sciences, P. Debyelaan 25, P.O. Box 5800, 6202 AZ, Maastricht, The Netherlands*

Received 10 May 2012; received in revised form 29 June 2012; accepted 15 September 2012

KEYWORDS
Prenatal stress;
Depression;
Anxiety;
Microarray;
Resilience;
Epigenetics

Abstract
Adverse life events during pregnancy may impact upon the developing fetus, predisposing prenatally stressed offspring to the development of psychopathology. In the present study, we examined the effects of prenatal restraint stress (PS) on anxiety- and depression-related behavior in both male and female adult Sprague-Dawley rats. In addition, gene expression profiles within the hippocampus and frontal cortex (FC) were examined in order to gain more insight into the molecular mechanisms that mediate the behavioral effects of PS exposure.
PS significantly increased anxiety-related behavior in male, but not female offspring. Likewise, depression-related behavior was increased in male PS rats only. Further, male PS offspring showed increased basal plasma corticosterone levels in adulthood, whereas both PS males and

*Corresponding author at: Department of Neuroscience, School for Mental Health and Neuroscience (MHeNS), Maastricht University, European Graduate School of Neuroscience (EURON), Universiteitssingel 50, P.O. Box 616, 6200 MD, Maastricht, The Netherlands. Tel.: +31 43 3884120; fax: +31 43 3671096.
E-mail address: d.vandenhove@maastrichtuniversity.nl (D.L.A. Van den Hove).
[1]These authors contributed equally to this work.

0924-977X/$ - see front matter
http://dx.doi.org/10.1016/j.euroneuro.2012.09.011

females had lower stress-induced corticosterone levels when compared to controls. Microarray-based profiling of the hippocampus and FC showed distinct sex-dependent changes in gene expression after PS. Biological processes and/or signal transduction cascades affected by PS included glutamatergic and GABAergic neurotransmission, mitogen-activated protein kinase (MAPK) signaling, neurotrophic factor signaling, phosphodiesterase (PDE)/ cyclic nucleotide signaling, glycogen synthase kinase 3 (GSK3) signaling, and insulin signaling. Further, the data indicated that epigenetic regulation is affected differentially in male and female PS offspring. These sex-specific alterations may, at least in part, explain the behavioral differences observed between both sexes, i.e. relative vulnerability versus resilience to PS in male versus female rats, respectively. These data reveal novel potential targets for antidepressant and mood stabilizing drug treatments including PDE inhibitors and histone deacetylase (HDAC) inhibitors.

1. Introduction

Environmental adversity, either physical or emotional, experienced by the mother during pregnancy, may impact upon the developing fetus, adversely affecting its physical and mental wellbeing in later life. In humans, prenatal stress (PS) has been associated with the development of various cognitive and affective disorders, such as depression and anxiety (Huizink et al., 2004; Van den Bergh et al., 2005; Weinstock, 2001). Likewise, PS in rats has been associated with altered stress responsivity and increased anxiety- and depression-related behavior, see review by Huizink et al. (2004). These behavioral effects of PS can be counteracted by treating prenatally stressed rat offspring with various kinds of antidepressants (Alonso et al., 1999; Morley-Fletcher et al., 2003a, 2004; Poltyrev et al., 2005; Poltyrev and Weinstock, 2004). Therefore, PS in rats is regarded as a valid 'etiological' animal model to obtain more insight into the pathophysiology of affective disorders.

Similar to the human situation, the effects of PS exposure in rats are highly sex-dependent. More specifically, PS in Sprague-Dawley rats has been shown to particularly affect male offspring, whereas females are relatively resilient at the behavioral level (Zuena et al., 2008). Along similar lines, e.g. the hippocampus – a brain structure that is subject to sex-dependent development and is well-known for its role in affective regulation – has been shown to be differentially affected by PS in male and female rat offspring, which is indicative of sex-specific vulnerability to disturbed glutamatergic and GABAergic neurotransmission and reduced hippocampal neuroplasticity (e.g. Zuena et al., 2008; Morley-Fletcher et al., 2011; Laloux et al., 2012).

In the present study, we examined the effects of PS in both male and female Sprague-Dawley rats. Adult anxiety- and depression-related behavior was studied using the elevated zero maze test, the home cage emergence test, the forced swim test, and the sucrose intake test. Further, basal and stress-induced activity of the hypothalamus-pituitary-adrenal (HPA) axis was studied. Finally, we examined the effects of PS on gene expression profiles within the hippocampus and frontal cortex (FC), two brain regions known to be critically involved in the pathophysiology of depressive disorders and the response to antidepressant treatment (Sheline et al., 2003; Taylor et al., 2008). For this purpose, as a *hypothesis-generating* approach, a whole genome microarray-based design was used in order to identify the genes and related molecular pathways that mediate vulnerability versus resilience to the behavioral effects of developmental stress exposure in male and female PS offspring, respectively.

2. Experimental procedures

2.1. Animals and procedures

This study was approved by the Animal Ethics Board of the Maastricht University, The Netherlands. Acclimatized Sprague-Dawley rats (Charles River, The Netherlands) were used. The animals were housed individually within a temperature-controlled environment (21 ± 1 °C) with a 12 h light/12 h dark cycle (lights on from 7.00–19.00 h) and had access to standard rat chow and water ad libitum. Pregnancy was determined by observation of vaginal plugs (embryonic day 0–E0). Restraint stress was performed daily during the last week of pregnancy (E14–E21). Pregnant female rats (n=8) were individually restrained 3 times a day (at approximately 9.00, 13.00, and 17.00 h) for 45 min in transparent plastic cylinders, whilst being exposed to bright light (Van den Hove et al., 2005; Ward and Weisz, 1984). Control (C) pregnant females (n=8) were left undisturbed in their home cages. Only litters of 8 or more pups were included in this study. Litters were culled to 8 pups if necessary. A maximum of 2 male and female pups per litter were examined to prevent litter effects (Chapman and Stern, 1978).

At postnatal day 21 (P21), pups were weaned and group-housed for further examination (2 male or 2 female rats/cage; n=14 rats per experimental condition per sex). Rats were kept at a reversed day-night cycle from this point onwards (lights on from 17.00–5.00 h). Anxiety- and depression-related behavior of the rats was analyzed from P120 onwards (in the order as discussed below). Subsequently, at P143, plasma corticosterone secretion was assessed. One week later, at P150, the animals were killed by quick decapitation, after which the brains were removed. The hippocampus and FC were dissected, weighed and bilateral tissue samples were placed in a single tube and snapshot frozen in liquid nitrogen after which they were stored at −80 °C until further analysis.

2.2. Anxiety- and depression-related behavior

The elevated zero maze (EZM) introduced by Shepherd et al. (1994) consisted of a circular alley (diameter of 100 cm; path width 10 cm) made from black plastic material that was transparent for infrared light and elevated 20 cm above the floor. The maze was divided into four parts, i.e., two opposite open parts and two opposite closed parts with sidewalls 30 cm in height. The open parts had borders with a height of 5 mm to prevent the rat from stepping down from the apparatus. For the test, the rat was placed into one of the open

parts facing a closed part of the apparatus. After 5 min the rat was removed from the apparatus and the maze was cleaned with ethanol (70%) and water and dried thoroughly. The movements of the rat were scored automatically under dark conditions with a computerized system using an infrared video camera (Ethovision Pro, Noldus, The Netherlands). Percentage of time spent in the open part of the maze and total distance traveled were determined.

In the home cage emergence (HCE) test the rat's home cage (opened) was placed in the center of an open field (1 m^2; under low light conditions) and the rat was allowed to leave its cage via a grid walkway. The latency to emerge from the home cage (i.e., four paws on the grid) was scored. If the rat did not emerge from its home cage within 300 s, the session was ended, the home cage was closed again and the rat was given a score of 300 s. The scores of 3 trials carried out on 3 consecutive days were averaged (Prickaerts et al., 1996).

In the forced swimming test (FST), originally designed by Porsolt et al. (1978), four cylindrical glass tanks (50 cm tall, 20 cm in diameter) were filled to a height of 30 cm with 25 °C water. The movements of the rat were scored automatically with a computerized system (Ethovision Pro, Noldus, The Netherlands) during a 5 min session under low light conditions. Scored were 'immobility', which reflects no movement at all and/or minor movements necessary to keep the nose above the water, and 'strong mobility', reflecting 'escape behavior' (e.g. climbing against the walls and diving). Settings within Ethovision were adjusted based on manually recorded sessions and were attuned for each sex separately (immobility/mobility threshold: 12 and 20; mobility/strong mobility threshold: 16.5 and 23.9 for males and females, respectively; Strackx et al., 2009).

The sucrose intake (SI) test was used to examine anhedonia (Willner et al., 1992; Dalla et al., 2005; Gronli et al., 2005). Rats were allowed to acclimatize to a 1% sucrose solution 2 days before the actual experiment. At 5.00 h on the test day, at the start of the dark phase, rats were deprived of food and water for 14 h. At 19.00 h, i.e., 2 h after the lights had turned on a 1% sucrose solution was offered. After 1 h sucrose consumption was measured and the intake was expressed in ml 1% sucrose/kg body weight consumed to control for intake differences due to possible differences in body weight (Dalla et al., 2005; Gronli et al., 2005).

2.3. Corticosterone response and radioimmuno-assay

To test the HPA axis responsivity, rats were individually placed in a type II (mouse) cage filled with 500 ml 25 °C water. Experiments were performed in an isolated room between 13.00 and 15.00 h. Immediately after taking the rat from its home cage, a first blood sample was collected via a saphenous vein puncture representing the basal corticosterone level. Immediately after this first sample was taken, the rat was put in the cage filled with water for 20 min after which a second blood sample was taken. Afterwards, the animal was returned to its home cage and left undisturbed for 40 min after which a final blood sample was taken. Blood samples were kept on ice and centrifuged at 5000 rpm for 10 min at 4 °C, after which the plasma was frozen down to −75 °C for subsequent determination of corticosterone levels (in duplicate). For this purpose, 50 μl of plasma was extracted with 3 ml dichloromethane and vortexed for 1 min. Corticosterone was subsequently measured directly on 1 ml dried dichloromethane and extracted for radioimmunoassay using corticosterone-^{125}I. The radioimmunological reaction was performed overnight at 4 °C, after which a second antibody system was used to separate bound and unbound steroid as previously described in detail (Sulon et al., 1978). The average intra- and inter-assay coefficients of variation for all assays were below 10%. The assay had a sensitivity of 7.7 ng/mL.

2.4. RNA preparation

Total RNA was extracted using RNeasy Mini kits (QIAGEN, Venlo, The Netherlands). Glass beads of 1 mm together with buffer RLT (provided by the RNeasy Mini kit) were added to the frozen tissues, and subsequently homogenized in a Minibead Beater (Biospec Products, OK, USA). After removal of cellular debris by centrifugation, extraction was continued according to instructions of the RNeasy Mini kit.

2.5. Microarray hybridization

Analysis of whole genome expression was performed at the facilities of ServiceXS (Leiden, The Netherlands). Quality of RNA samples was assessed by electrophoresis using the Agilent 2100 Bioanalyzer (Agilent Technologies, Santa Clara, CA, USA). Of each experimental group four pools of three samples were prepared. Pools were subsequently hybridized on the RatRef-12 Expression BeadChip (Illumina, San Diego, CA, USA).

2.6. Data normalization

Normalization of expression data was performed as previously described (Alttoa et al., 2010). In summary, the raw microarray data were processed using the Beadarray (Dunning et al., 2007) PreprocessCore (Bolstad et al., 2003) and PUMA (Sanguinetti et al., 2006) R packages of bioconductor (Bioconductor). In the Beadarray package the BackgroundCorrect method used was ''minimum'', whilst variables for the CreatebeadsummaryData method were as follows: log=TRUE, n=10. Data were normalized using the quantile normalization algorithm from the PreprocessCore package. An important outcome measure of the PUMA analysis is the Probability of Positive Log Ratio (pplr) statistic, a probability measure of differential expression that considers uncertainty of expression levels. Statistically significant differentially expressed genes were defined as genes with a minimum pplr value (the minimum of pplr or 1−pplr) less than 0.001. As such, separate sets of differentially expressed genes between control and PS animals for each gender and brain region (hippocampus and FC) were generated.

2.7. Microarray data analysis

To find significantly over-represented molecular pathways within the sets of genes differentially regulated by PS, we searched the pathway database of the Kyoto Encyclopedia of Genes and Genomes (KEGG) using the DAVID Functional Annotation Tool (http://david.abcc.ncifcrf.gov/, see also (Huang da et al., 2009)). The KEGG pathway database is a collection of manually drawn graphical diagrams that represent the current knowledge of molecular interactions involved in various cellular processes (http://www.genome.ad.jp/kegg/pathway.html). The DAVID tool produces a gene enrichment score (EASE score, which is a modified Fisher Exact p-value) for each KEGG pathway. For identifying significant enriched pathways the cut-off value was set at $P<0.05$. Additionally, the lists of differentially expressed genes were manually screened to identify genes encoding proteins, known to be implicated in signaling pathways in the pathophysiology and/or treatment of mood disorders.

2.8. Statistical analysis

EZM, FST and SI data were explored by using a two-way ANOVA (sex x condition). In addition, since all of these tests displayed either a significant sex x condition interaction effect and/or highly significant sex effects, a stratified analysis was performed for each sex separately. For the HCE test, the data were not normally distributed

since some rats remained in the home cage for the entire observation period. Therefore, these data were transformed to rank scores, after which average escape latencies were compared between groups. Plasma corticosterone values were ln-transformed to normality. HCE data and corticosterone levels were analyzed by a repeated measures ANOVA (sex x condition) and also independently at the different time points using a two-way ANOVA (sex x condition). Correlation analysis was performed using Pearson's correlation coefficient (r_p). Statistical significance was assumed to exist at $P<0.05$, except when studying the effects of PS on corticosterone levels at the individual time points, in order to correct for multiple testing ($P<0.017$). All statistics were carried out using SPSS software version 12.0.1 (SPSS Inc, USA).

3. Results

3.1. Maternal weight gain, offspring birth weight, litter size and pre-weaning mortality

Maternal stress exposure in this cohort of animals was associated with reduced maternal weight gain over gestation, concomitant with impaired fetal growth in both sexes, as reported previously (Van den Hove et al., 2010). No differences were observed in litter size (13.6±0.9 and 14.1±0.5 pups per litter for C and PS, respectively) or pre-weaning mortality (no pups died in either group after litters had been culled to 8 pups).

3.2. Anxiety- and depression-related behavior

The percentage of time spent in the open arms of the EZM as well as the distance covered in the EZM are depicted in Figure 1. An overall sex x condition interaction was observed ($F_{1,49}=6.662$; $P=0.013$) as well as an overall sex-effect ($F_{1,49}=5.983$; $P=0.018$). The overall condition effect did not reach statistical significance ($F_{1,49}=2.050$; $P=0.159$). Stratified analyses showed that PS male rats spent less time in the open arms of the EZM as compared to C males (PS effect: −34.4%, $F_{1,24}=7.557$; $P=0.011$). In addition, an overall sex-effect for the total distance moved in the EZM was found ($F_{1,49}=18.369$; $P<0.001$), whereas there was no overall condition-effect or sex x condition interaction ($F_{1,49}=1.491$; $P=0.228$ and $F_{1,49}=3.587$; $P=0.064$, respectively). Stratified analysis revealed that male PS rats covered less distance during the 5 min trial as compared to C males (PS effect: −25.3%, $F_{1,24}=4.970$; $P=0.035$). No differences were observed between PS and C females in this respect ($F_{1,25}=0.704$; $P=0.409$ for time spent in the open arms, and $F_{1,25}=0.222$; $P=0.642$ for total distance moved). The average escape latencies in the HCE test are shown in Figure 2. Over time, a significant overall effect for PS was found ($F_{1,48}=6.423$; $P=0.015$) as well as a significant sex effect ($F_{1,48}=49.482$; $P<0.001$). The sex x condition interaction effect over time, however, failed to reach statistical significance ($F_{1,48}=0.031$; $P=0.860$). More specifically, over the three trials, male PS rats took more time to leave the home cage as compared to controls (PS effect: +25.3%, $F_{1,25}=4.863$; $P=0.037$). A similar trend was observed in female offspring, although this was not significance (PS effect: +33.7%, $F_{1,23}=3.026$; $P=0.095$). Results from the FST are shown in Figure 3. The immobility time did not show overall PS effects, nor did it show a sex x condition

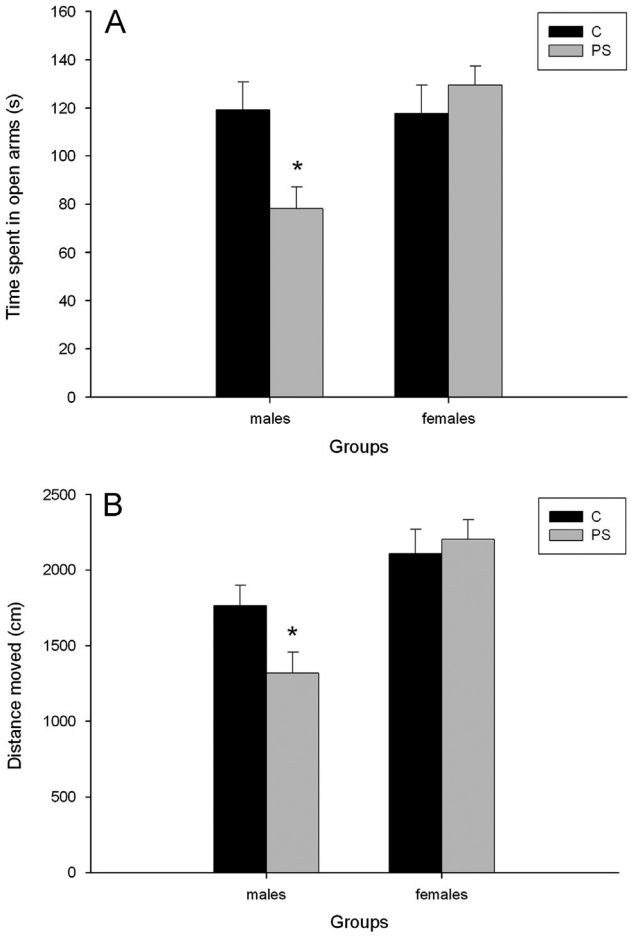

Figure 1 Percentage of time spent in the open arms of (A) and total distance moved in (B) the elevated zero maze (EZM). Values represent means+S.E.M. Male prenatally stressed (PS) rats spent less time in the open arms of the EZM as compared to control (C) males. Further, male PS rats covered less distance during the 5 min trial as compared to C males. No differences were observed between PS and C females. *$P<0.05$ (One-way ANOVA).

interaction ($F_{1,52}=0.957$; $P=0.333$ and $F_{1,52}=0.309$; $P=0.581$, respectively). However, a profound overall sex effect was observed ($F_{1,52}=69.658$; $P<0.001$), while stratified analysis per sex revealed no differences between PS and controls (males: $F_{1,26}=0.807$; $P=0.377$; females: $F_{1,26}=0.164$; $P=0.688$). Strong mobility in the FST showed an overall trend ($F_{1,52}=3.239$; $P=0.078$), a highly significant sex effect ($F_{1,52}=16.952$; $P<0.001$) and a trend for a sex x condition interaction ($F_{1,52}=3.466$; $P=0.068$). Stratified analysis indicated that PS in males resulted in less strong mobility as compared to controls (PS effect: −21.7%, $F_{1,26}=4.241$; $P<0.05$), whereas no differences in strong mobility were observed between female groups ($F_{1,26}=0.005$; $P=0.947$). Overall, no differences in SI were observed between PS and C offspring ($F_{1,24}=2.401$; $P=0134$). While there was no sex x condition interaction ($F_{1,24}=0.422$; $P=0.522$), a significant overall sex effect was found ($F_{1,24}=11.158$; $P=0.003$). Stratified analysis showed no differences between PS and control offspring in either sex (males: $F_{1,12}=0.619$; $P=0.447$; females: $F_{1,12}=1.796$; $P=0.205$) (Table 1).

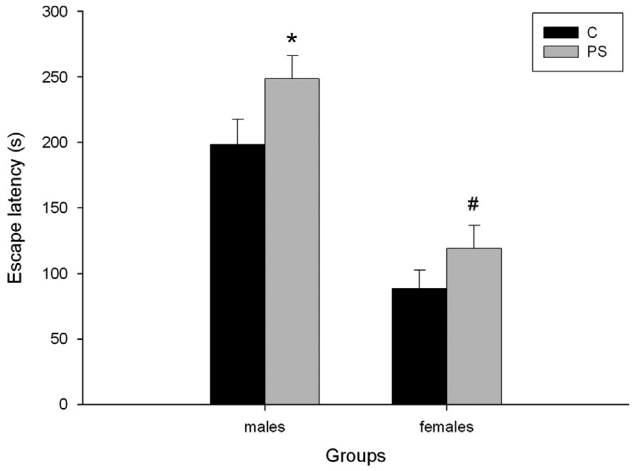

Figure 2 Average escape latencies in the home cage emergence (HCE) test. Values represent means (s)+S.E.M. Over the three trials, male prenatally stressed (PS) rats took more time to leave the home cage as compared to controls (C). A similar pattern was observed in female offspring, though this did not reach statistical significance. $^{*}P<0.05$, $^{\#}0.05<P<0.10$ (ANOVA based on ranks).

3.3. Corticosterone response

Plasma corticosterone levels under basal conditions, immediately after 20 min of restraint stress, or 40 min after being placed back into the home cage, are depicted in Figure 4. Analysis with repeated-measures ANOVA revealed a highly significant change in corticosterone levels over time ($F_{2,90}=128.375$; $P<0.001$; sphericity assumptions met), as well as a significant overall PS effect ($F_{1,45}=4.947$; $P=0.031$) and a highly significant overall sex effect ($F_{1,45}=33.591$; $P<0.001$), whereas the sex x condition interaction was not significant ($F_{1,45}=0.353$; $P=0.555$). Looking at the three measurements individually (two-way ANOVA) indicated overall PS effects for basal corticosterone levels ($F_{1,45}=9.871$; $P=0.003$) and stress levels ($F_{1,45}=14.194$; $P<0.001$), both of which were accompanied by highly significant sex differences ($F_{1,45}=40.632$; $P<0.001$ for basal levels and $F_{1,45}=73.856$; $P<0.001$ for stress levels). Overall condition effects for recovery after stress were, however, not significant ($F_{1,45}=2.511$; $P=0.120$) and showed no sex or sex x treatment interaction effects ($F_{1,45}=0.016$; $P=0.900$ and $F_{1,45}=0.102$; $P=0.751$, respectively). Stratified analysis revealed a significant within-subjects effect in males both for time ($F_{2,50}=83.926$; $P<0.001$) and experimental group x time ($F_{2,50}=7.803$; $P=0.001$). In addition, over time, a significant effect of PS was observed ($F_{1,25}=4.933$; $P=0.036$). Male PS rats further showed higher basal plasma corticosterone levels as compared to controls (PS effect: +108.7%, $F_{1,25}=11.568$; $P=0.002$), whereas stress-induced corticosterone levels were again lower in male PS rats (PS effect: −21.9%, $F_{1,25}=10.183$; $P=0.004$). In females, a significant within-subjects effect was observed only for time ($F_{2,40}=65.937$; $P<0.001$). Further, only stress-induced plasma corticosterone levels differed between groups, with PS females showing lower corticosterone levels as compared to controls (PS effect: −21.6%, $F_{1,20}=4.876$; $P=0.039$). No difference between groups was observed after 40 min of recovery (males: $F_{1,25}=0.846$; $P=0.367$; females: $F_{1,20}=1.768$; $P=0.199$).

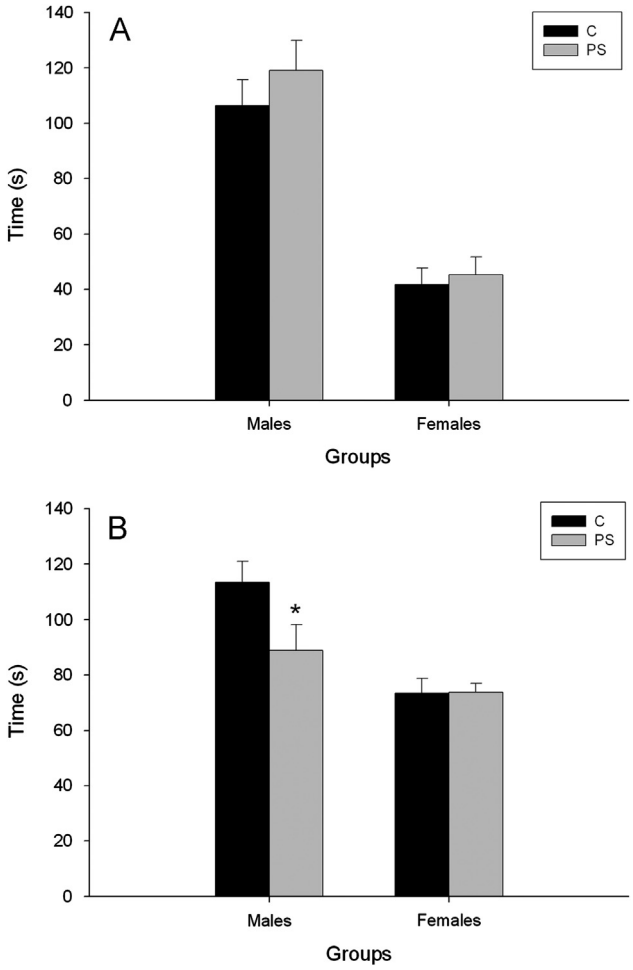

Figure 3 Immobility (A) and strong mobility (B) in the forced swim test (FST); Values represent means (s)+S.E.M. Whereas no differences between groups were observed in time spent immobile, prenatal stress (PS) in males resulted in less strong mobility as compared to controls (C). No differences in any parameter were observed between female groups. $^{*}P<0.05$ (One-way ANOVA).

Table 1 Sucrose intake (ml/kg body weight).

Sex	Group	Sucrose intake
Males	**C**	39.5±4.7
	PS	45.1±5.4
Females	**C**	56.6±6.8
	PS	70.1±7.6

Values represent means±S.E.M. Abbreviations: C: control and PS: prenatal stress. No significant differences between experimental groups were observed.

3.4. Brain region weights

Weight data of the hippocampus and FC are listed in Table 2. Relative hippocampal weight was higher in PS females as

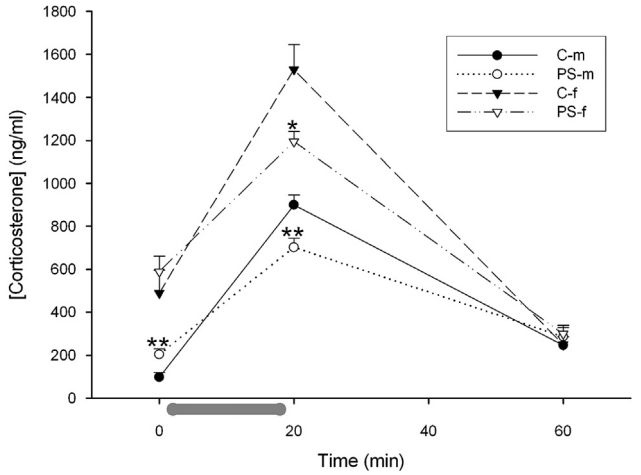

Figure 4 Stress-induced corticosterone secretion. Values represent means (ng/ml)+S.E.M. Male prenatally stressed (PS) rats showed higher basal plasma corticosterone levels as compared to controls (C). Stress-induced corticosterone levels (the grey bar represents a 20 min period of stress) were lower in both male and female PS offspring. No difference between groups was observed 40 min after placing the animals back into their home cage. $^{*}P<0.05$, $^{**}P<0.01$ (One-way ANOVA).

Table 2 Brain region weights (mg/kg body weight).

Sex	Group	Hippocampus	FC
Males	C	302.9±9.8	79.2±4.7
	PS	299.4±9.8	95.4±6.4
Females	C	485.9±14.5	147.1±5.6
	PS	550.1±19.8[a]	164.6±15.1

Values represent means±S.E.M. Abbreviations: C: control, PS: prenatal stress and FC: frontal cortex.
[a] $P<0.05$ (Student's *t*-test).

compared to C females (PS effect: 13.2%, $P=0.015$). No difference between groups was observed in any other case.

3.5. Gene expression profiles

3.5.1. Differential expression of genes related to stress and affective behavior

Within the hippocampus, PS affected the expression of 44 and 1084 genes in male and female offspring, respectively. Within the FC, 114 and 688 genes were expressed differentially by PS in male and female offspring, respectively. An overview of all genes regulated by PS exposure within the hippocampus and FC of male offspring is given in Tables 3 and 4, respectively. Individual genes regulated in the hippocampus and FC of female offspring is depicted in Supplemental Material S1 and S2.

3.5.2. Pathway analyses

DAVID-KEGG analysis showed that in male offspring no KEGG pathways were significantly enriched by PS within any of the brain regions, which was related to the limited number of genes affected by PS in male offspring. Results from the KEGG pathway analyses on gene expression profiles within the female hippocampus and FC are depicted in Tables 5 and 6, respectively. Within the hippocampus, 'cell adhesion molecules (CAMs)', 'ErbB signaling pathway', 'focal adhesion', 'insulin signaling pathway', 'long term potentiation', 'mTOR signaling pathway', 'phosphatidylinositol (PI) signaling system', and 'tight junction' were significantly changed after PS. Within the FC, the KEGG pathways 'ribosome' and 'Wnt-signaling' were significantly affected by PS. In addition, manual browsing of the gene lists for candidate genes encoding proteins known to be involved in the pathophysiology and/or treatment of affective disorders revealed several differentially expressed genes involved in glutamate and gamma-aminobutyric acid (GABA) neurotransmission, cyclic adenosine monophosphate (cAMP)/ cyclic guanosine monophosphate (cGMP)/ phosphodiesterase (PDE) signaling, and epigenetic regulation, in both the hippocampus and FC of male and female PS offspring (see Table 7). An overview on relevant signaling cascades altered within the female hippocampus and FC, based on the expression profiles and subsequent functional clustering using DAVID is given in Figure 5.

4. Discussion

As a hypothesis-generating approach, in order to gain more insight into the molecular mechanisms that mediate the behavioral effects of developmental stress exposure, we examined the enduring effects of PS exposure on gene expression profiles within the hippocampus and FC of adult male and female Sprague-Dawley rats. While PS increased anxiety- and depression-related behavior particularly in male Sprague-Dawley rats, female offspring seemed to be relatively resilient to PS exposure. In addition, PS altered the expression of numerous genes in the hippocampus and FC in a sex-specific manner. These sex-specific alterations may, at least in part, explain the behavioral differences observed between both sexes, i.e. relative vulnerability versus resilience to PS in male versus female rats, respectively.

4.1. Sex differences in behavior and the response to stress

PS resulted in a significant increase in anxiety- and depression-related behavior in male offspring, while behavior in females was largely unaffected. In addition, only male PS offspring showed clearly increased basal plasma corticosterone levels, whereas PS offspring of both sexes failed to show an adequate response to stress. Among females, adult hippocampal weight was relatively increased after PS.

Although the overall prevalence of mood disorders is higher in female as compared to male humans (Blehar, 1995), a different pattern seems to be observed in PS-related psychopathology (Darnaudery and Maccari, 2007). Whereas only male PS Sprague-Dawley rats showed a clear increase in anxiety- and depression-related behavior, PS females seemed to remain relatively resilient to PS exposure in the present study. Studies by the group of

Table 3 Genes differentially regulated by PS exposure in the male hippocampus, sorted by fold change.

Entrez symbol	Entrez gene ID	Gene name	Transcript	Probe ID	Fold change
Mrpl18_predicted	292244	mitochondrial ribosomal protein L18	ILMN_54513	ILMN_1359180	5.46
Sc5dl	114100	sterol-C5-desaturase (ERG3 delta-5-desaturase homolog, *S. cerevisiae*)-like	ILMN_263006	ILMN_1363277	2.59
Rbj	298859	rab and DnaJ domain containing	ILMN_278305	ILMN_1355125	1.31
Kcnab2	29738	potassium voltage-gated channel, shaker-related subfamily, beta member 2	ILMN_267848	ILMN_1355212	1.28
mrpl11	293666	mitochondrial ribosomal protein L11	ILMN_291563	ILMN_1363330	1.28
Ttyh3_predicted	304315	tweety homolog 3 (Drosophila)	ILMN_272392	ILMN_1651087	1.27
Trrap_predicted	288471	transformation/transcription domain-associated protein	ILMN_267735	ILMN_1360742	1.25
Hdac4_predicted	363287	histone deacetylase 4	ILMN_266642	ILMN_1364573	1.24
LOC361990	361990	similar to DKFZP547E1010 protein; similar to Protein C1orf77 homolog	ILMN_66762	ILMN_1650076	1.21
Thg1l	303067	tRNA-histidine guanylyltransferase 1-like (*S. cerevisiae*)	ILMN_286909	ILMN_1649860	1.20
RGD1307814_predicted	362559	zyg-11 homolog B (*C. elegans*)	ILMN_278965	ILMN_1375196	1.19
Rhcg	293048	Rh family, C glycoprotein	ILMN_281613	ILMN_1361451	1.19
RGD1565184_predicted	502705	similar to VEPH isoform A	ILMN_48005	ILMN_1530385	1.17
LOC501534	501534	NA	ILMN_66173	ILMN_1360820	1.16
RGD1566402_predicted	500127	homeo box A10	ILMN_285373	ILMN_1354843	1.16
Farsb	301544	phenylalanyl-tRNA synthetase, beta subunit	ILMN_265522	ILMN_1356564	1.15
Ibrdc2_predicted	364681	ring finger protein 144B	ILMN_291094	ILMN_1366789	1.15
Lgals7	29518	lectin, galactoside-binding, soluble, 7	ILMN_297724	ILMN_1376402	1.15
Mrc2_predicted	295631	phospholipase A2 receptor 1	ILMN_277146	ILMN_1358009	1.15
Spn	24796	Sialophorin	ILMN_279075	ILMN_1361495	1.15
Dnajc11_predicted	362666	DnaJ (Hsp40) homolog, subfamily C, member 11	ILMN_62144	ILMN_1361685	1.14
Sbk1	113907	similar to SH3-binding kinase; SH3-binding domain kinase 1	ILMN_284727	ILMN_1353425	1.14
LOC503147	503147	similar to FLJ45949 protein	ILMN_66420	ILMN_1361222	1.13
Wdr7	66031	WD repeat domain 7	ILMN_290962	ILMN_1351953	1.13
LOC500878	500878	similar to LRRGT00057	ILMN_48959	ILMN_1372001	1.11
Calr3_predicted	364529	calreticulin 3	ILMN_48314	ILMN_1375963	0.89
Dhh	84380	desert hedgehog homolog (Drosophila)	ILMN_53576	ILMN_1370554	0.89
Mif	81683	macrophage migration inhibitory factor (MIF)	ILMN_264813	ILMN_1356539	0.89
Olr1491_predicted	404969	olfactory receptor 1491	ILMN_277212	ILMN_1359277	0.89
Aspn	306805	asporin	ILMN_285309	ILMN_1369408	0.88
Pik3c2g	116720	phosphoinositide-3-kinase, class 2, gamma polypeptide	ILMN_273653	ILMN_1349959	0.88
Lhx6_predicted	311901	LIM homeobox 6	ILMN_60425	ILMN_1352539	0.87
Ufd1l	84478	ubiquitin fusion degradation 1 like (yeast)	ILMN_49407	ILMN_1372253	0.87
Sema6b	84609	sema domain, transmembrane domain (TM), and cytoplasmic domain, (semaphorin) 6B	ILMN_288957	ILMN_1650011	0.86
Limk1	65172	LIM domain kinase 1	ILMN_286066	ILMN_1372778	0.85
Traf3ip3	360900	TRAF3 interacting protein 3	ILMN_287167	ILMN_1365920	0.85
Olr556	405249	olfactory receptor 557; olfactory receptor 556	ILMN_269876	ILMN_1373130	0.84
Timm9	171139	translocase of inner mitochondrial membrane 9 homolog (yeast)	ILMN_271875	ILMN_2039665	0.83
Gnl3	290556	guanine nucleotide binding protein-like 3 (nucleolar); similar to guanine nucleotide binding protein-like 3 (nucleolar)	ILMN_263704	ILMN_1357924	0.80
Mrps2_predicted	362094	mitochondrial ribosomal protein S2	ILMN_50349	ILMN_1365807	0.80
Prim2	301323	primase, DNA, polypeptide 2	ILMN_270579	ILMN_1355020	0.80
Arsb	25227	arylsulphatase B	ILMN_58825	ILMN_1366780	0.73

Table 4 Genes differentially regulated by PS exposure in the male FC, sorted by fold change.

Symbol	Entrez gene ID	Gene name	Transcript	Probe ID	Fold change
Mrpl18_predicted	292244	mitochondrial ribosomal protein L18	ILMN_54513	ILMN_1359180	6.40
Sc5dl	114100	sterol-C5-desaturase (ERG3 delta-5-desaturase homolog, *S. cerevisiae*)-like	ILMN_263006	ILMN_1363277	2.00
C4-2	406161	complement component 4, gene 2	ILMN_271471	ILMN_1361837	1.31
Txnip	117514	thioredoxin interacting protein	ILMN_280023	ILMN_1359696	1.29
Prim1	246327	DNA primase, p49 subunit	ILMN_271101	ILMN_1353345	1.28
Gng11	64199	guanine nucleotide binding protein (G protein), gamma 11	ILMN_62822	ILMN_1354189	1.25
Plac8_predicted	360914	placenta-specific 8	ILMN_292070	ILMN_1363160	1.24
Tmem140	362334	transmembrane protein 140	ILMN_278563	ILMN_1372260	1.24
Cyyr1	304138	cysteine/tyrosine-rich 1	ILMN_287228	ILMN_1374917	1.22
Ifitm3	361673	interferon induced transmembrane protein 3	ILMN_265471	ILMN_1352762	1.22
Heph	117240	Hephaestin	ILMN_269859	ILMN_1371544	1.21
Lcp1	306071	lymphocyte cytosolic protein 1	ILMN_279425	ILMN_1376765	1.20
Commd9	295956	COMM domain containing 9	ILMN_270917	ILMN_1370105	1.19
LOC309349	309349	SLIT and NTRK-like family, member 2	ILMN_65982	ILMN_1357725	1.19
Cyba	79129	cytochrome b-245, alpha polypeptide	ILMN_279326	ILMN_1366276	1.18
Gpm6a	306439	glycoprotein m6a	ILMN_280628	ILMN_1367162	1.18
Loxl1	315714	lysyl oxidase-like 1	ILMN_267667	ILMN_1376846	1.18
Tnfrsf11b	25341	tumor necrosis factor receptor superfamily, member 11b	ILMN_285163	ILMN_1374220	1.18
Slc37a1	294321	solute carrier family 37 (glycerol-3-phosphate transporter), member 1	ILMN_297940	ILMN_1376690	1.15
Sox17_predicted	312936	SRY (sex determining region Y)-box 17	ILMN_288748	ILMN_1359017	1.15
Ssg1	64387	coiled-coil domain containing 80	ILMN_59129	ILMN_1362820	1.15
Loxl2_predicted	290350	lysyl oxidase-like 2	ILMN_55682	ILMN_1351352	1.14
Slpi	84386	secretory leukocyte peptidase inhibitor	ILMN_270427	ILMN_1360286	1.14
Fxyd5	60338	FXYD domain-containing ion transport regulator 5	ILMN_274559	ILMN_1371590	1.13
Ms4a11_predicted	361735	membrane-spanning 4-domains, subfamily A, member 11	ILMN_295413	ILMN_1356010	1.13
LOC363259	363259	obscurin-like 1	ILMN_52302	ILMN_1351812	1.12
Ninj2	59115	ninjurin 2	ILMN_289402	ILMN_1370725	1.12
Rdm1_predicted	287726	RAD52 motif 1	ILMN_64467	ILMN_1363012	1.12
RGD1560542_predicted	499847	proline rich Gla (G-carboxyglutamic acid) 4 (transmembrane)	ILMN_277969	ILMN_1650382	1.12
RT1-S2	24994	RT1 class Ib, locus H2-TL-like (S2)	ILMN_264682	ILMN_1368215	1.12
Timeless	83508	timeless homolog (Drosophila)	ILMN_275078	ILMN_1370013	1.12
LOC497832	497832/ 89821	transient receptor potential cation channel, subfamily C, member 1	ILMN_64900	ILMN_1373735	1.11
RGD1561935_predicted	502180	similar to hypothetical protein 4930474N05	ILMN_283847	ILMN_1367261	1.11
Arhgap21_predicted	307178	Rho GTPase activating protein 21	ILMN_280800	ILMN_1364451	1.10
Hhex	79237	hematopoietically expressed homeobox	ILMN_280416	ILMN_1353851	1.10
LOC498331	498331	protein tyrosine phosphatase, non-receptor type 13	ILMN_286408	ILMN_1365973	1.10
Nr1h3	58852	nuclear receptor subfamily 1, group H, member 3	ILMN_269442	ILMN_1352599	1.10
RGD1562979_predicted	305501	similar to DNA-binding protein Ikaros form 1 - mouse	ILMN_56783	ILMN_1367066	1.10
LOC364321	364321	similar to T-cell receptor alpha-chain precursor	ILMN_65095	ILMN_1649960	1.09
RGD1310868_predicted	303702	endo-beta-N-acetylglucosaminidase	ILMN_64738	ILMN_1368424	1.08
Slc9a1	24782	solute carrier family 9 (sodium/hydrogen exchanger), member 1	ILMN_283430	ILMN_1363067	1.08
Hdgf	114499	hepatoma-derived growth factor	ILMN_299659	ILMN_1358138	1.07
RGD1560568_predicted	500914	basic transcription factor 3; similar to basic transcription factor 3	ILMN_68049	ILMN_1359066	1.06
Hp1bp3	313647	heterochromatin protein 1, binding protein 3	ILMN_297506	ILMN_1362886	0.94
Sf3b2_predicted	293671	splicing factor 3b, subunit 2	ILMN_276631	ILMN_1363457	0.94
RGD1565310_predicted	362697	similar to RIKEN cDNA 1110018J12	ILMN_298926	ILMN_1349900	0.93
Trim27_predicted	291171	tripartite motif-containing 27	ILMN_287365	ILMN_1374685	0.93
Calcb	171519	calcitonin-related polypeptide, beta	ILMN_291051	ILMN_1369359	0.92

Table 4 (*continued*)

Symbol	Entrez gene ID	Gene name	Transcript	Probe ID	Fold change
RGD1305500_predicted	308004	similar to hypothetical protein FLJ13188	ILMN_69760	ILMN_1357698	0.92
40428	64551	septin 7	ILMN_277931	ILMN_1370494	0.91
Atp6v1b2	117596	ATPase, H transporting, lysosomal V1 subunit B2	ILMN_265715	ILMN_1360084	0.91
Iqcb1_predicted	303915	IQ motif-containing B1	ILMN_268980	ILMN_1367093	0.91
Ntrk2	25054	neurotrophic tyrosine kinase, receptor, type 2	ILMN_302906	ILMN_1366426	0.91
Oact2	313997	membrane bound O-acyltransferase domain containing 2	ILMN_287627	ILMN_1373404	0.91
RGD1559475_predicted	498977	similar to dynactin 3; dynactin 3	ILMN_270142	ILMN_1350986	0.91
RGD1564628_predicted	302566	ubiquitin specific peptidase 27, X-linked	ILMN_265296	ILMN_1350769	0.91
Stap1	305269	signal transducing adapter family member 1	ILMN_265181	ILMN_1369894	0.91
Tmem18	362722	transmembrane protein 18	ILMN_291730	ILMN_1367804	0.91
Tsnax	64028	translin-associated factor X	ILMN_275146	ILMN_1352444	0.91
Cd19_predicted	365367	CD19 molecule	ILMN_55073	ILMN_1367276	0.90
Ddx47	297685	DEAD (Asp-Glu-Ala-Asp) box polypeptide 47	ILMN_282637	ILMN_1350598	0.90
Eif3d	362952	eukaryotic translation initiation factor 3, subunit D	ILMN_273976	ILMN_1650977	0.90
Hars2_predicted	362227	D-tyrosyl-tRNA deacylase 1 homolog (*S. cerevisiae*)	ILMN_61958	ILMN_1364969	0.90
Mrps5_predicted	296134	mitochondrial ribosomal protein S5	ILMN_54617	ILMN_1358174	0.90
Npat_predicted	315666	nuclear protein, ataxia-telangiectasia locus	ILMN_56219	ILMN_1366007	0.90
RGD1309216	361726	similar to hypothetical protein FLJ20487	ILMN_269528	ILMN_1361771	0.90
RGD1561681_predicted	498661	similar to Pyruvate kinase isozymes M1/M2 (Pyruvate kinase muscle isozyme)	ILMN_286284	ILMN_1374660	0.90
Tmprss2	156435	transmembrane protease, serine 2	ILMN_280888	ILMN_1353103	0.90
V1ra12	297439	vomeronasal 1 receptor, A12	ILMN_265037	ILMN_1368051	0.90
Bbx_predicted	303970	bobby sox homolog (Drosophila)	ILMN_57321	ILMN_1368994	0.89
Chchd4	312559	coiled-coil-helix-coiled-coil-helix domain containing 4; similar to coiled-coil-helix-coiled-coil-helix domain containing 4	ILMN_278959	ILMN_1350912	0.89
Foxp1_predicted	297480	forkhead box P1	ILMN_64445	ILMN_1351093	0.89
Ipo9_predicted	304817	importin 9	ILMN_276568	ILMN_1353713	0.89
LOC500936	500936	RGD1560018	ILMN_57948	ILMN_1368595	0.89
Ncor1	54299	nuclear receptor co-repressor 1	ILMN_296119	ILMN_1357958	0.89
RGD1311456_predicted	363089	family with sequence similarity 63, member B	ILMN_52033	ILMN_1354049	0.89
RGD1311756_predicted	362769	similar to hypothetical protein FLJ20950	ILMN_263635	ILMN_1356092	0.89
Rp9h_predicted	363032	retinitis pigmentosa 9 (human)	ILMN_266474	ILMN_1650578	0.89
Tcf15_predicted	296272	transcription factor 15	ILMN_294039	ILMN_1364142	0.89
Tmem158	117582	transmembrane protein 158	ILMN_282420	ILMN_1371878	0.89
Ash2l_predicted	290829	ash2 (absent, small, or homeotic)-like (Drosophila)	ILMN_275112	ILMN_1361125	0.88
Cdk105	171456	similar to TGF beta-inducible nuclear protein 1 (L-name related LNR42); CDK105 protein	ILMN_288993	ILMN_2039008	0.88
Ipmk	171458	similar to inositol polyphosphate multikinase; inositol polyphosphate multikinase	ILMN_267871	ILMN_1355219	0.88
LOC500483	500483	RGD1559893	ILMN_59110	ILMN_1650108	0.88
Mafb	54264	v-maf musculoaponeurotic fibrosarcoma oncogene homolog B (avian)	ILMN_272535	ILMN_1361027	0.88
Pscd3	116693	cytohesin 3	ILMN_64245	ILMN_1355570	0.88
Bhlhb2	79431	basic helix-loop-helix family, member e40	ILMN_291562	ILMN_1374180	0.87
Exosc9	294975	exosome component 9	ILMN_281173	ILMN_1362725	0.87
Papola_predicted	314417	poly (A) polymerase alpha	ILMN_269256	ILMN_1367021	0.87
Gsk3b	84027	glycogen synthase kinase 3 beta	ILMN_283436	ILMN_1349648	0.86
LOC308976	308976	jumonji domain containing 5	ILMN_54422	ILMN_1370490	0.86
Pftk1_predicted	362316	PFTAIRE protein kinase 1	ILMN_57754	ILMN_1355708	0.86
Pou3f2	29588	POU class 3 homeobox 2	ILMN_61074	ILMN_1370881	0.86
Gabra4	140675	gamma-aminobutyric acid (GABA) A receptor, alpha 4	ILMN_282396	ILMN_1363867	0.85
Galnt2_predicted	292090	UDP-N-acetyl-alpha-D-galactosamine:polypeptide N-acetylgalactosaminyltransferase 2 (GalNAc-T2)	ILMN_287371	ILMN_1355124	0.85
Grm5	24418	glutamate receptor, metabotropic 5	ILMN_292416	ILMN_1361607	0.85
Ktn1_predicted	361029	kinectin 1	ILMN_48977	ILMN_1354299	0.85

Table 4 (*continued*)

Symbol	Entrez gene ID	Gene name	Transcript	Probe ID	Fold change
LOC363410	363410	similar to Ras-related protein Rab-27B	ILMN_54002	ILMN_1370567	0.85
LOC500950	500950	zinc finger protein 317	ILMN_67762	ILMN_1351340	0.85
RGD1311340_predicted	309243	vacuolar protein sorting 13 homolog A (*S. cerevisiae*)	ILMN_65042	ILMN_1372429	0.85
RGD1311723_predicted	363018	similar to KIAA1731 protein	ILMN_66607	ILMN_1360056	0.85
Tra1_predicted	362862	tumor rejection antigen gp96	ILMN_284286	ILMN_1376625	0.85
Cpsf2_predicted	299256	cleavage and polyadenylation specific factor 2	ILMN_49851	ILMN_1373200	0.84
Keap1	117519	Kelch-like ECH-associated protein 1	ILMN_289150	ILMN_1366907	0.83
Kpnb1	24917	karyopherin (importin) beta 1	ILMN_276390	ILMN_1373492	0.83
RGD1562526_predicted	499821	family with sequence similarity 171, member B	ILMN_54084	ILMN_1365584	0.82
Grin2a	24409	glutamate receptor, ionotropic, N-methyl D-aspartate 2A	ILMN_290907	ILMN_1376686	0.81
RGD1561386_predicted	500985	Cas-Br-M (murine) ecotropic retroviral transforming sequence	ILMN_291557	ILMN_1355687	0.79
Trak2	171086	trafficking protein, kinesin binding 2	ILMN_54675	ILMN_1352978	0.78
LOC497742	497742/ 361745	SWI/SNF related, matrix associated, actin dependent regulator of chromatin, subfamily a, member 2	ILMN_69842	ILMN_1349796	0.77
Arsb	25227	arylsulphatase B	ILMN_58825	ILMN_1366780	0.71
Hpcal4	50872	hippocalcin-like 4	ILMN_287235	ILMN_1373628	0.67

Morley-Fletcher et al. (2003a,b), which use the same PS model, i.e. repetitive restraint stress in Sprague-Dawley rats, illustrate a similar pattern with males showing a more vulnerable behavioral phenotype (Darnaudery and Maccari, 2007; Zuena et al., 2008). In addition to the increased vulnerability of males towards, for example, the development of an anxious phenotype, their latest study actually showed PS females to be less anxious as compared to control female offspring, i.e. two even more distinct behavioral phenotypes. The more distinct phenotype might be explained by the fact that Zuena and colleagues started restraining their pregnant dams from 11 days of gestation onwards. Furthermore, Zuena et al. (2008) studied the offspring at a younger age, i.e., 3 months. In line with these sex-specific behavioral phenotypes, prenatally stressed male Sprague-Dawley rats show impaired hippocampal plasticity, whereas female rats exposed to PS show signs of increased structural plasticity (Darnaudery and Maccari, 2007). Discrepancies between these findings and those from other groups may be explained by the use of other rat strains and/or maternal stress paradigms; an issue that has already been addressed recently (Zuena et al., 2008). Further, the age of the offspring studied may play an important role as well. The sex-dependent effects of PS are probably related to the sex-specific timing of relevant developmental processes over gestation (e.g., Owen and Matthews, 2003). The exact role of sex in relation to PS remains to be elucidated though.

4.2. Age-related differences in HPA axis (re-)activity

Similarly, the observed pattern of stress-induced corticosterone secretion in our study was substantially different from that of other investigations in Sprague-Dawley rats using the same PS model, but offspring of a different age. In a study by Morley-Fletcher et al. (2003a) using male Sprague-Dawley rats of 3 months of age, no effect of PS on either basal or stress-induced plasma corticosterone levels was found. In that study, however, recovery after 20 min of restraint stress was weaker after PS. In two other comparable studies by the same group using male Sprague-Dawley rats of 2 months of age, both stress-induced plasma corticosterone levels as well as levels after recovery were higher in PS animals (Dugovic et al., 1999; Morley-Fletcher et al., 2003b). An age-dependent relationship between adverse early-life experience (maternal deprivation) and HPA axis (re-)activity was already suggested by De Kloet and Oitzl (2003). Though different in nature, a comparable phenomenon seems to be involved in HPA axis (re-)activity after PS. We therefore hypothesize that alterations in HPA axis (re-)activity per se, rather than just HPA axis hyperactivity are of importance in relation to PS exposure.

4.3. Gene expression profiles

Microarray analysis revealed various region- and sex-specific effects of PS. Whereas the behavioral effects of PS were more pronounced in male offspring, gene expression was altered to a greater extent in female offspring. Relevant genes affected in male offspring that may explain, at least in part, the behavioral alterations induced by PS, include those encoding for Mrpl18 and Sc5dl (both of which were highly increased in both the hippocampus and FC), TrkB (decreased expression within the FC), hippocalcin (decreased expression within the FC) and HDAC4 (increased expression within the hippocampus). Concerning the female offspring, we hypothesize that the increased number of differentially expressed genes reflects an adaptive response to PS, involving mechanisms that contribute to resilience to the pro-depressant effects of PS. Biological processes and/or signal transduction cascades affected by PS in female offspring

Table 5 KEGG pathways and associated genes regulated by PS exposure in the female hippocampus.

Entrez symbol	Entrez gene ID	Gene name	Transcript	Probe ID	Fold change
Cell adhesion molecules (CAMs)					
Alcam	79559	activated leukocyte cell adhesion molecule	ILMN_298443	ILMN_1370154	0.34
Cd226_predicted	307199	cd226 antigen (predicted)	ILMN_58791	ILMN_1350388	1.14
Cd276	315716	b7 homolog 3	ILMN_61049	ILMN_1360321	1.36
Cd80	25408	cd80 antigen	ILMN_300031	ILMN_1353891	1.15
Cldn10_predicted	290485	claudin 10 (predicted)	ILMN_272711	ILMN_1358030	0.70
Cldn5	65131	claudin 5	ILMN_63515	ILMN_1352195	1.19
Cntn2	25356	contactin 2	ILMN_295743	ILMN_1367489	1.35
Itga6	114517	integrin; alpha 6	ILMN_285522	ILMN_1351793	0.78
Ncam1	24586	neural cell adhesion molecule 1	ILMN_284523	ILMN_1370085	0.48
Negr1	59318	neuronal growth regulator 1	ILMN_289426	ILMN_1366196	0.39
Nlgn1	116647	neuroligin 1	ILMN_298217	ILMN_1364761	1.27
Nrxn1	60391	neurexin 1	ILMN_263241	ILMN_1369278	0.53
Pdcd1_predicted	301626	programmed cell death 1 (predicted)	ILMN_269125	ILMN_1357025	1.16
RT1-Ba	309621	butyrophilin-like 2 (mhc class ii associated)	ILMN_302329	ILMN_1376669	1.48
RT1-S3	294228	rt1 class ib; locus bm1	ILMN_275620	ILMN_1371428	1.47
Sdc4	24771	syndecan 4	ILMN_284660	ILMN_1352387	1.36
ErbB signaling					
Camk2b	24245	calcium/calmodulin-dependent protein kinase ii beta subunit	ILMN_295816	ILMN_1367246	0.37
Cblb	171136	casitas b-lineage lymphoma b	ILMN_290443	ILMN_1351226	0.50
Crk	54245	v-crk sarcoma virus ct10 oncogene homolog (avian)	ILMN_265349	ILMN_1361978	0.68
Egf	25313	epidermal growth factor	ILMN_284600	ILMN_1371224	1.15
Egfr	24329	epidermal growth factor receptor	ILMN_268935	ILMN_1362571	0.79
Elk1	314436	elk1; member of ets oncogene family	ILMN_56253	ILMN_1651026	0.71
Kras	24525	kirsten rat sarcoma viral oncogene homolog 2 (active)	ILMN_284143	ILMN_1373027	0.65
Map2k2	58960	mitogen activated protein kinase kinase 2	ILMN_273342	ILMN_1362844	1.32
Mapk1	116590	mitogen activated protein kinase 1	ILMN_267006	ILMN_1349290	0.66
Pak3	29433	p21 (cdkn1a)-activated kinase 3	ILMN_283805	ILMN_1373238	0.40
Pik3cb	85243	phosphatidylinositol 3-kinase; catalytic; beta polypeptide	ILMN_296182	ILMN_1368644	0.82
Pik3r3	60664	phosphatidylinositol 3 kinase; regulatory subunit; polypeptide 3	ILMN_268148	ILMN_1358018	0.57
Rps6kb2	361696	ribosomal protein s6 kinase; polypeptide 2	ILMN_275356	ILMN_1370952	1.29
Focal adhesion					
Actg_predicted	287876	actin; gamma; cytoplasmic	ILMN_55178	ILMN_1362269	0.78
Cav1	25404	caveolin	ILMN_288688	ILMN_1376388	0.63
Crk	54245	v-crk sarcoma virus ct10 oncogene homolog (avian)	ILMN_265349	ILMN_1361978	0.68
Egf	25313	epidermal growth factor	ILMN_284600	ILMN_1371224	1.15
Egfr	24329	epidermal growth factor receptor	ILMN_268935	ILMN_1362571	0.79
Elk1	314436	elk1; member of ets oncogene family	ILMN_56253	ILMN_1651026	0.71
Flnb_predicted	306204	filamin; beta (predicted)	ILMN_64302	ILMN_1362723	0.83
Itga10_predicted	310683	integrin; alpha 10 (predicted)	ILMN_274071	ILMN_1373558	1.18
Itga6	114517	integrin; alpha 6	ILMN_285522	ILMN_1351793	0.78
Mapk1	116590	mitogen activated protein kinase 1	ILMN_267006	ILMN_1349290	0.66
Pak3	29433	p21 (cdkn1a)-activated kinase 3	ILMN_283805	ILMN_1373238	0.40
Pdgfd	66018	platelet-derived growth factor; d polypeptide	ILMN_299016	ILMN_1352347	0.90
Pdpk1	81745	3-phosphoinositide dependent protein kinase-1	ILMN_276807	ILMN_1359177	0.28
Pik3cb	85243	phosphatidylinositol 3-kinase; catalytic; beta polypeptide	ILMN_296182	ILMN_1368644	0.82
Pik3r3	60664	phosphatidylinositol 3 kinase; regulatory subunit; polypeptide 3	ILMN_268148	ILMN_1358018	0.57
Vtn	29169	vitronectin	ILMN_291791	ILMN_1374141	1.29
Insulin signaling					
Acaca	60581	acetyl-coenzyme a carboxylase alpha	ILMN_264748	ILMN_1374107	0.78

Table 5 (*continued*)

Entrez symbol	Entrez gene ID	Gene name	Transcript	Probe ID	Fold change
Cblb	171136	casitas b-lineage lymphoma b	ILMN_290443	ILMN_1351226	0.50
Crk	54245	v-crk sarcoma virus ct10 oncogene homolog (avian)	ILMN_265349	ILMN_1361978	0.68
Elk1	314436	elk1; member of ets oncogene family	ILMN_56253	ILMN_1651026	0.71
Ins1	24505	insulin 1	ILMN_66664	ILMN_1370839	1.13
Kras	24525	kirsten rat sarcoma viral oncogene homolog 2 (active)	ILMN_284143	ILMN_1373027	0.65
Map2k2	58960	mitogen activated protein kinase kinase 2	ILMN_273342	ILMN_1362844	1.32
Mapk1	116590	mitogen activated protein kinase 1	ILMN_267006	ILMN_1349290	0.66
Pdpk1	81745	3-phosphoinositide dependent protein kinase-1	ILMN_276807	ILMN_1359177	0.28
Pik3cb	85243	phosphatidylinositol 3-kinase; catalytic; beta polypeptide	ILMN_296182	ILMN_1368644	0.82
Pik3r3	60664	phosphatidylinositol 3 kinase; regulatory subunit; polypeptide 3	ILMN_268148	ILMN_1358018	0.57
Rps6kb2	361696	ribosomal protein s6 kinase; polypeptide 2	ILMN_275356	ILMN_1370952	1.29
Long-term potentiation (LTP)					
Camk2b	24245	calcium/calmodulin-dependent protein kinase ii beta subunit	ILMN_295816	ILMN_1367246	0.37
Gnaq	81666	guanine nucleotide binding protein; alpha q polypeptide	ILMN_280496	ILMN_1355584	0.48
Grm5	24418	glutamate receptor; metabotropic 5	ILMN_292416	ILMN_1361607	0.71
Kras	24525	kirsten rat sarcoma viral oncogene homolog 2 (active)	ILMN_284143	ILMN_1373027	0.65
LOC317203	317203	similar to ribosomal protein s6 kinase polypeptide 6	ILMN_68494	ILMN_1374028	0.82
Map2k2	58960	mitogen activated protein kinase kinase 2	ILMN_273342	ILMN_1362844	1.32
Mapk1	116590	mitogen activated protein kinase 1	ILMN_267006	ILMN_1349290	0.66
Ppp3ca	24674	protein phosphatase 3; catalytic subunit; alpha isoform	ILMN_271084	ILMN_1372414	0.45
mTOR signaling					
Ins1	24505	insulin 1	ILMN_66664	ILMN_1370839	1.13
LOC317203	317203	similar to ribosomal protein s6 kinase polypeptide 6	ILMN_68494	ILMN_1374028	0.82
Mapk1	116590	mitogen activated protein kinase 1	ILMN_267006	ILMN_1349290	0.66
Pdpk1	81745	3-phosphoinositide dependent protein kinase-1	ILMN_276807	ILMN_1359177	0.28
Pik3cb	85243	phosphatidylinositol 3-kinase; catalytic; beta polypeptide	ILMN_296182	ILMN_1368644	0.82
Pik3r3	60664	phosphatidylinositol 3 kinase; regulatory subunit; polypeptide 3	ILMN_268148	ILMN_1358018	0.57
Rps6kb2	361696	ribosomal protein s6 kinase; polypeptide 2	ILMN_275356	ILMN_1370952	1.29
Phosphatidylinositol (PI) signaling					
Impa1	83523	inositol (myo)-1(or 4)-monophosphatase 1	ILMN_302173	ILMN_1364531	0.85
LOC497681	25666/ 497681	diacylglycerol kinase, gamma	ILMN_56964	ILMN_1363234	0.43
Pik3c2a_predicted	361632	phosphatidylinositol 3-kinase; c2 domain containing; alpha polypeptide (predicted)	ILMN_264548	ILMN_1361702	0.57
Pik3c2g	116720	phosphatidylinositol 3-kinase; c2 domain containing; gamma polypeptide	ILMN_273653	ILMN_1349959	1.14
Pik3cb	85243	phosphatidylinositol 3-kinase; catalytic; beta polypeptide	ILMN_296182	ILMN_1368644	0.82
Pik3r3	60664	phosphatidylinositol 3 kinase; regulatory subunit; polypeptide 3	ILMN_268148	ILMN_1358018	0.57
Pip4k2b	89812	phosphatidylinositol-4-phosphate 5-kinase; type ii; beta	ILMN_291864	ILMN_1349115	0.63
Synj1	85238	synaptojanin 1	ILMN_59553	ILMN_1355054	0.50
Tight junction function					
Actg_predicted	287876	actin; gamma; cytoplasmic	ILMN_55178	ILMN_1362269	0.78
Cldn10_predicted	290485	claudin 10 (predicted)	ILMN_272711	ILMN_1358030	0.70
Cldn5	65131	claudin 5	ILMN_63515	ILMN_1352195	1.19
Epb4.1l1	59317	erythrocyte protein band 4.1-like 1	ILMN_267921	ILMN_1376582	0.81

Table 5 (*continued*)

Entrez symbol	Entrez gene ID	Gene name	Transcript	Probe ID	Fold change
Hcls1	288077	hematopoietic cell specific lyn substrate 1	ILMN_272174	ILMN_1376482	1.18
Kras	24525	kirsten rat sarcoma viral oncogene homolog 2 (active)	ILMN_284143	ILMN_1373027	0.65
Magi2	113970	activin receptor interacting protein 1	ILMN_276385	ILMN_1369780	0.61
Myh13	29605	myosin; heavy polypeptide 13; skeletal muscle	ILMN_301178	ILMN_1360194	1.13
Myh3	24583	myosin; heavy polypeptide 3; skeletal muscle; embryonic	ILMN_302443	ILMN_1360458	1.44
Pard6g_predicted	307237	par-6 partitioning defective 6 homolog gamma (*C. elegans*) (predicted)	ILMN_53782	ILMN_1650781	0.85
Prkce	29340	protein kinase c; epsilon	ILMN_294755	ILMN_1373193	0.32

include glutamatergic and GABAergic neurotransmission, MAPK/CREB signaling, cAMP/cGMP/PDE signaling, GSK3B signaling, IP signaling, and central insulin signaling. Further, epigenetic regulation seemed to be affected to a different degree in both male and female offspring exposed to PS. These findings may indicate new potential therapeutic targets in the treatment of affective disorders. Below we will discuss the role of several biological processes in more detail.

4.3.1. Glutamate and GABA

The observed gene expression profiles suggest a significant role for glutamatergic neurotransmission in mediating the effects of PS. For example, female offspring exposed to PS showed a decrease in the expression of the ionotropic N-methyl D-aspartate (NMDA) receptors 1 and 2A within the FC, as well as a decreased metabotropic glutamate receptor 5 (mGluR5) expression in both the hippocampus and FC. Recent evidence has suggested that altered glutamatergic neurotransmission, which may have its origin in early development, plays an important role in the pathophysiology of mood disorders (Hashimoto, 2009a, 2009b). Both the NMDA and mGlu receptors have been proposed as potential therapeutic targets in this respect (Pilc et al., 2008; Pittenger et al., 2007). Pilc et al. (2008) suggested a model in which mGlu5 antagonists may possess antidepressant activity through NMDA receptor blockade. Likewise, the observed decrease in mGlu5 receptor expression within both the hippocampus and FC, together with the observed decrease in the expression of the NMDA1 and 2A receptors within the FC of female offspring exposed to PS, may relate to the resilience towards PS in this sex. Whether these changes represent a compensatory response to the decreased expression of glutamic acid decarboxylase (GAD; decreased in both the hippocampus and FC of PS females), the enzyme that catalyzes the decarboxylation of glutamate to GABA, remains to be elucidated. In a recent investigation by Zuena et al. (2008), PS was shown to result in a reduction in mGlu5 receptor protein levels within the hippocampus of male offspring only. These rats further showed increased anxiety-related behavior. In contrast, female PS rats in that same study displayed reduced anxiety and no change in mGlu5 receptor levels in the hippocampus. The authors suggested that the decrease in mGlu receptor function observed in PS male rats represents "an unsuccessful homeostatic mechanism aimed at restoring the physiological levels of the anxiety response" (Zuena et al., 2008). Though mRNA expression is markedly different from protein expression, the discrepancy between their study and ours may further be explained by the fact that the rats used in our study are older as compared to those in the study by Zuena et al. (2008).

Closely related to glutamate function is the role of the inhibitory neurotransmitter GABA and its receptors. Dysfunction of the GABAergic neurotransmitter system has recently been associated with the development of both mood and anxiety disorders (Kalueff and Nutt, 2007; Price et al., 2009). Moreover, in both human and animal studies, positive modulators of GABAergic neurotransmission generally exert anxiolytic and antidepressant effects, while negative modulators possess anxiogenic- or depressive-like activity (Kalueff and Nutt, 2007). It is known that stress as well as many GABAergic psychotropic drugs is both capable of affecting GABA receptor subunit composition, which in turn may dramatically affect its functions (Zhang et al., 1998). Similarly, the expression of multiple GABAergic receptor subunits was affected after PS in the present study. For example, within the FC of male offspring, the expression of the alpha 4 subunit was decreased in PS as compared to control animals. Within females, the expression of various GABA receptor subunits was affected by PS in both brain regions. Further, as mentioned above, the expression of GAD was decreased in both the hippocampus and FC of PS females.

Altogether, these data suggest that changes in glutamatergic and GABAergic neurotransmission may play a prominent role in the regulation of affective state and reiterate the need for further research on their possible therapeutic value in disorders like anxiety and depression.

4.3.2. Ribosome function

The Mrpl18 gene encodes a 39S subunit protein that belongs to the L18P ribosomal protein family, the exact function of which remains largely unknown. Recently though, Mrpl18 has been shown to play a key role in mediating import of the nuclear DNA-encoded 5S rRNA into mitochondria, by which 5S rRNA molecules can be specifically withdrawn from the cytosolic pool and redirected to mitochondria, bypassing the classic nucleolar reimport pathway (Smirnov et al., 2011). The profound increase in Mrpl18 mRNA expression in

Table 6 KEGG pathways and associated genes regulated by PS exposure in the female FC.

Entrez symbol	Entrez gene ID	Gene name	Transcript	Probe ID	Fold change
Ribosome function					
LOC501605	501605	ribosomal protein s2	ILMN_68333	ILMN_1364624	1.60
LOC684988	684988	ribosomal protein s13	ILMN_263434	ILMN_1351503	1.24
LOC690364	690364	ribosomal protein l21	ILMN_274137	ILMN_1363975	1.23
RGD1563431_predicted	501876	large subunit ribosomal protein l36a	ILMN_296283	ILMN_2040666	1.25
RGD1564290_predicted	498837	ribosomal protein s27a	ILMN_68667	ILMN_1362582	1.16
Rpl18a	290641	similar to 60s ribosomal protein l18a	ILMN_285160	ILMN_1370927	1.25
Rpl24	64307	ribosomal protein l24	ILMN_283110	ILMN_1353774	1.18
Rpl37	81770	ribosomal protein l37	ILMN_284909	ILMN_1354107	1.33
Rpl7	297755	ribosomal protein l7	ILMN_281851	ILMN_1370118	1.29
Rps11	81774	ribosomal protein s11	ILMN_288262	ILMN_1373412	1.25
Rps23	124323	ribosomal protein s23	ILMN_263631	ILMN_1369998	1.61
Rps7	29258	ribosomal protein s7	ILMN_62060	ILMN_1650594	1.26
Rps8	65136	ribosomal protein s8	ILMN_266152	ILMN_1362384	1.11
Wnt signaling					
Camk2b	24245	calcium/calmodulin-dependent protein kinase ii beta subunit	ILMN_295816	ILMN_1367246	0.81
Camk2g	171140	calcium/calmodulin-dependent protein kinase ii gamma	ILMN_290091	ILMN_1364240	0.88
Chd8	65027	beta-catenin binding protein	ILMN_53502	ILMN_1363589	0.80
Ctnnb1	84353	catenin (cadherin associated protein); beta 1; 88 kda	ILMN_297571	ILMN_1352752	1.31
Cxxc4	83824	cxxc finger 4	ILMN_273940	ILMN_1350191	0.85
Gsk3b	84027	glycogen synthase kinase 3 beta	ILMN_283436	ILMN_1349648	0.81
Lrp6_predicted	312781	low density lipoprotein receptor-related protein 6 (predicted)	ILMN_278789	ILMN_1349678	0.86
Map3k7_predicted	313121	mitogen activated protein kinase kinase kinase 7 (predicted)	ILMN_265678	ILMN_1371190	1.16
Ppard	25682	peroxisome proliferator activated receptor delta	ILMN_272514	ILMN_1357865	0.88
Ppp3cb	24675	protein phosphatase 3; catalytic subunit; beta isoform	ILMN_263806	ILMN_1351926	1.22

both the hippocampus and FC of PS male offspring, in addition to the altered expression of related genes, e.g. Mrpl11 and Mrps2 (both in FC), as well as Mrps5 and Ms4a11 (both in hippocampus) suggests a dysregulated transport of 5s rRNA and associated ribosomal function.

Interestingly, PS increased the expression of numerous genes encoding ribosomal proteins in the FC of female offspring (13 differentially expressed, all of which increased by PS exposure). This suggests that the brain is increasing its capacity for protein synthesis, which could be interpreted as an attempt to compensate for impaired cytosolic translation (Bonow et al., 2009).

4.3.3. MAPK/CREB/neurotrophic factor signaling and hippocalcin

DAVID analysis showed a substantial overall negative effect of PS on MAPK signaling within the female hippocampus. Examples of genes downregulated by PS within this brain region were genes for the rat sarcoma viral oncogene homolog 2 (RAS), calcineurin (CaN), MAPK 1 (or ERK2), MAPK kinase kinase 1 (MAP3K1 or MEKK1), and ribosomal s6 kinase (RSK). Furthermore, the expression of the gene encoding for MAPK phosphatase-4 (MKP4), also known as dual specificity phosphatase 9 (DUSP9), which is known to deactivate MAPK, was increased in PS females.

A major substrate for the ERK/MAPK signaling pathway is the transcription factor CREB, which regulates the expression of, e.g. BDNF and is known to play an important role in mediating the antidepressant effects of neurotrophic factors and growth factors (Schmidt and Duman, 2011; Tanis et al., 2007). Interestingly, impaired function of BDNF and its receptor, the tyrosine kinase B (TrkB) receptor, have been linked to the development of major depression as well as a diminished response to antidepressant drugs (Dong et al., 2009; Duman and Monteggia, 2006; Tanis and Duman, 2007; Tanis et al., 2007). In the present study, Ntrk2 gene expression (which encodes the TrkB receptor) was decreased by PS in the FC of male offspring. CREB signaling can also be induced by Ca^{2+}-calmodulin-regulated kinases

Table 7 Overview of differentially expressed genes related to glutamatergic and GABAergic neurotransmission, cAMP/cGMP/PDE signaling, and epigenetic regulation, in the hippocampus and FC of male and female PS offspring.

Entrez symbol	Area	Sex	Entrez gene ID	Gene name	Transcript	Probe ID	Fold change
Glutamatergic/ GABAergic neurotransmission							
Gabra1	HIP	f	29705	gamma-aminobutyric acid (GABA) A receptor, alpha 1	ILMN_53178	ILMN_1348806	0.60
Gabrb1	HIP	f	25450	gamma-aminobutyric acid (GABA) A receptor, beta 1	ILMN_274145	ILMN_1357628	0.53
Gabbr1	HIP	f	81657	gamma-aminobutyric acid (GABA) B receptor 1	ILMN_60885	ILMN_1354454	0.64
Gad2	HIP	f	24380	glutamate decarboxylase 2	ILMN_296357	ILMN_1371012	0.67
Grm5	HIP	f	24418	glutamate receptor, metabotropic 5	ILMN_292416	ILMN_1361607	0.71
LOC289606	HIP	f	289606	gamma-aminobutyric acid (GABA) A receptor, alpha 2	ILMN_285601	ILMN_1352358	0.67
Grin2a	FC	m	24409	glutamate receptor, ionotropic, N-methyl D-aspartate 2A	ILMN_290907	ILMN_1376686	0.81
Grm5	FC	m	24418	glutamate receptor, metabotropic 5	ILMN_292416	ILMN_1361607	0.85
Gabrb1	FC	f	25450	gamma-aminobutyric acid (GABA) A receptor, beta 1	ILMN_274145	ILMN_1357628	0.89
Gad2	FC	f	24380	glutamate decarboxylase 2	ILMN_296357	ILMN_1371012	0.63
Grin1	FC	f	24408	glutamate receptor, ionotropic, N-methyl D-aspartate 1	ILMN_283876	ILMN_1365529	0.91
Grin2a	FC	f	24409	glutamate receptor, ionotropic, N-methyl D-aspartate 2A	ILMN_290907	ILMN_1376686	0.67
Grm5	FC	f	24418	glutamate receptor, metabotropic 5	ILMN_292416	ILMN_1361607	0.75
cAMP/cGMP/PDE signaling							
Pde4b	HIP	f	24626	phosphodiesterase 4B	ILMN_295710	ILMN_1353078	0.54
Pde7a	HIP	f	81744	phosphodiesterase 7A	ILMN_60421	ILMN_1353897	0.84
Pde8b	HIP	f	309962	phosphodiesterase 8B	ILMN_276608	ILMN_1348973	0.76
Pde10a	HIP	f	63885	phosphodiesterase 10A	ILMN_283323	ILMN_1361915	0.52
Pde2a	FC	f	81743	phosphodiesterase 2A	ILMN_278143	ILMN_1372916	0.76
Pde4b	FC	f	24626	phosphodiesterase 4B	ILMN_295710	ILMN_1353078	0.76
Epigenetic regulation							
Hdac4_predicted	HIP	m	363287	histone deacetylase 4	ILMN_266642	ILMN_1364573	1.24
Mbd1_predicted	HIP	f	291439	methyl-CpG binding domain protein 1	ILMN_51671	ILMN_1375594	0.71
Mettl2_predicted	HIP	f	363687	methyltransferase-like 2	ILMN_48481	ILMN_1370775	0.58
Hdac4_predicted	FC	f	363287	histone deacetylase 4	ILMN_266642	ILMN_1364573	0.77
Sirt2	FC	f	361532	sirtuin 2 (*S. cerevisiae*)	ILMN_281197	ILMN_1352401	1.30

f = female; m = male; HIP = hippocampus; and FC = frontal cortex.

(CAMKs), e.g., after stimulation of glutamatergic alpha-amino-3-hydroxy-5-methyl-4-isoxazolepropionic acid (AMPA) receptors (Tanis and Duman, 2007). Interestingly, the expression of CAMKII was decreased both within the hippocampus and FC of PS female as compared to control offspring. Further, the expression of *Gria 3*, encoding for the AMPA3 receptor, was decreased within the FC of PS females.

Hippocalcin, a member of the neuronal calcium sensor (NCS) protein family, is another protein involved in CREB signaling. Hippocalcin-deficient mice display a defect in CREB activation, associated with impaired spatial and associative memory (Kobayashi et al., 2005; Noguchi et al., 2007). In the present study, the expression of hippocalcin was decreased in the FC of male offspring exposed to PS, which may reflect impaired CREB-signaling in the FC of these animals.

4.3.4. GSK3B signaling

GSK-3B is implicated in the signaling pathways of various neurotransmitters and growth factors and has a repressing effect on transcription factors including CREB and B-catenin (Grimes and Jope, 2001; Salas et al., 2003). GSK-3B has been implicated in the etiology of various psychiatric disorders, such as major depression, schizophrenia, and bipolar disorder (Emamian et al., 2004; Gould et al., 2004b; Hur and Zhou, 2010; Li and Jope, 2010; Wada, 2009). The mood stabilizer lithium is a selective inhibitor of GSK-3 (Gould et al., 2004b). Data of rodent studies suggest that pharmacological inhibition of GSK-3 has antidepressant-like effects (Gould et al., 2004a; Kaidanovich-Beilin et al., 2004). In the present study, we observed a decrease in GSK-3B mRNA expression in the FC of both male and female PS offspring. In PS females though, GSK-3B mRNA expression was reduced to a greater extent as

compared to PS male offspring. In addition, the expression of B-catenin, one of the major downstream targets of GSK3B and the function of which is inhibited by GSK-3B activity, was increased substantially within the FC of PS females. Furthermore, the expression of *Chd8*, the gene encoding for B-catenin binding protein, which normally binds to B-catenin thereby inhibiting its function, was decreased, indicating an even more impaired GSK signaling in PS females. As such, impaired GSK-3B signaling may represent another interesting mechanism of action mediating resilience to PS in female offspring.

4.3.5. cAMP/cGMP/PDE signaling

Phosphodiesterases (PDEs) are enzymes that degrade the phosphodiester bond in the second messenger molecules cyclic adenosine monophosphate (cAMP) and/or cyclic guanosine monophosphate (cGMP) (Bender and Beavo, 2006). Within the hippocampus of PS female offspring, the expression of PDE4b, PDE7a, PDE8b and PDE10a was decreased. In addition, within the FC of PS females, the expression of PDE2a and PDE4b was reduced.

The inhibition of specific PDEs, which results in an increase in cAMP and/or cGMP dependent on the PDE type being inhibited, offers unique receptor-independent opportunities to modify cellular processes including apoptosis, differentiation, lipogenesis, glycogenolysis, gluconeogenesis and muscle contraction (Halene and Siegel, 2007). Thus, recently, PDE inhibitors have been identified as new potential therapeutics in areas such as dementia, depression, and schizophrenia (Halene and Siegel, 2007; Reneerkens et al., 2009; Tanis and Duman, 2007). The majority of the PDEs affected by PS degrade cAMP only, whereas PDE2 and PDE10 degrade both cAMP and cGMP. The cAMP system mediates the effect of monoamine neurotransmitters and is known to be downregulated in the brains of depressed patients (see review by Tanis and Duman, 2007). The depressive effect of impaired cAMP signaling is most likely related to the fact that cAMP activates protein kinase A (PKA), which, in turn, activates CREB. This notion is supported by the finding that chronic blockade of PDE4 with rolipram activates CREB and increases the expression of BDNF in the hippocampus, and that rolipram has antidepressant efficacy in both preclinical and clinical trials (Tanis and Duman, 2007). Along similar lines, it has been found that PDE4b−/− mice exhibited decreased immobility in the forced swimming test indicating an antidepressant-like effect (Zhang et al., 2008). PS male rat offspring in the present study showed increased depression-related behavior in the forced swimming test, whereas the behavior of PS female offspring was not affected as compared to control offspring. Thus, reduced levels of, e.g., PDE4b, as observed in PS female offspring in the present study, may explain the lack of depressive-like behavior in the forced swimming test in this sex after PS exposure. In this way, a decrease in PDE signaling may lead to increased cAMP/CREB signaling and related neurotrophic support. Expression levels of hippocampal PDE10a and FC PDE2a were reduced in PS females and, therefore, cGMP might also be of interest in mediating possible protective effects in PS females in the present study as it has recently been demonstrated that single nucleotide polymorphisms (SNPs) located in the genes encoding PDE2a, PDE10a, and the cGMP-specific PDE9a gene are associated with major depression (Wong et al., 2006).

Altogether, these data support the notion that specific PDE inhibitors might represent interesting candidates for possible treatment strategies for disorders such as major depression.

4.3.6. Central insulin signaling

In addition to its well-known role in peripheral glucose regulation, the hormone insulin has an important role in regulating central nervous system (CNS) function, the significance of which is underscored by the increased vulnerability to co-morbidities such as dementia and depression seen with insulin resistance and diabetes (Brown et al., 2004; Lustman and Clouse, 2005; McEwen et al., 2002; Ott et al., 1999). Interestingly, insulin and the insulin receptor (IR) have been shown to be produced in neurons throughout the brain (Devaskar et al., 1994; Zhao and Alkon, 2001), whilst particularly the hippocampus seems to be vulnerable to chronic hyperglycemia and insulin resistance (Reagan, 2007). The pathophysiological similarities between diabetes and mood disorders suggest that common mechanistic pathways may be involved in the etiology and progression of the neurological aspects of these disorders. For more information on the link between insulin signaling, memory and mood, (see Reagan, 2007; Robertson et al., 2010). Notably, our microarray data now also suggest a pivotal role for central insulin signaling in mediating the effects of PS. Within the female hippocampus, several genes linked to insulin and related PI signaling (Yang et al., 2008; Daimon et al., 2008; Aberg et al., 2006) were differentially expressed in PS offspring when compared to controls. Among others, the expression of *Ins1*, encoding for insulin itself, was upregulated. In addition, the hippocampal expression of *Slc2a3*, the gene encoding glucose transporter-3, which is responsible for the influx of glucose into neurons, was decreased in the same offspring. We therefore hypothesize that enhanced hippocampal insulin signaling in PS female offspring might represent a compensatory effect explaining why behavior in females was largely unaffected.

4.3.7. Epigenetic regulation

Recently, it has been suggested that epigenetic mechanisms may account for the symptoms of mental illness and their (partial) reversal during treatment (Krishnan and Nestler, 2008; McClung and Nestler, 2008; Mill and Petronis, 2007; Renthal and Nestler, 2009; Tsankova et al., 2007). Evidently, the use of PS as a developmental rat model for affective disorders is of particular interest in relation to epigenetic programming. Specifically, the endogenously programmed massive loss and subsequent re-establishment of DNA methylation in the embryo and fetus comprises diverse critical periods, during which environmental stimuli can affect epigenetic regulation (Waterland and Jirtle, 2004). In this respect, the expression patterns of various genes involved in epigenetic regulation are remarkable. For example, the expression of HDAC4 was upregulated within the hippocampus of PS male offspring, whereas it was downregulated within the FC of PS females. Other proteins involved in epigenetic regulation that are affected by PS are methyltransferase-like 2 and MBD1 (both downregulated

within the FC of PS females). Thus, it is likely that changes in epigenetic regulation in reaction to fetal distress may contribute to the various physiological and behavioral changes observed in prenatally stressed subjects. Recent studies in rodents already provided evidence for epigenetic programming by early prenatal maternal stress (Bale, 2011; Darnaudery and Maccari, 2007; Matrisciano et al., 2012; Morley-Fletche et al., 2011; Mueller and Bale, 2008; Zuena et al., 2008). Interestingly, recently, several studies have highlighted the antidepressant potential of HDAC inhibitors, although numerous challenges need to be addressed before being able to guarantee sufficient specificity, potency, and a benign side effect profile of this class of drugs (Covington et al., 2011; Grayson et al., 2010).

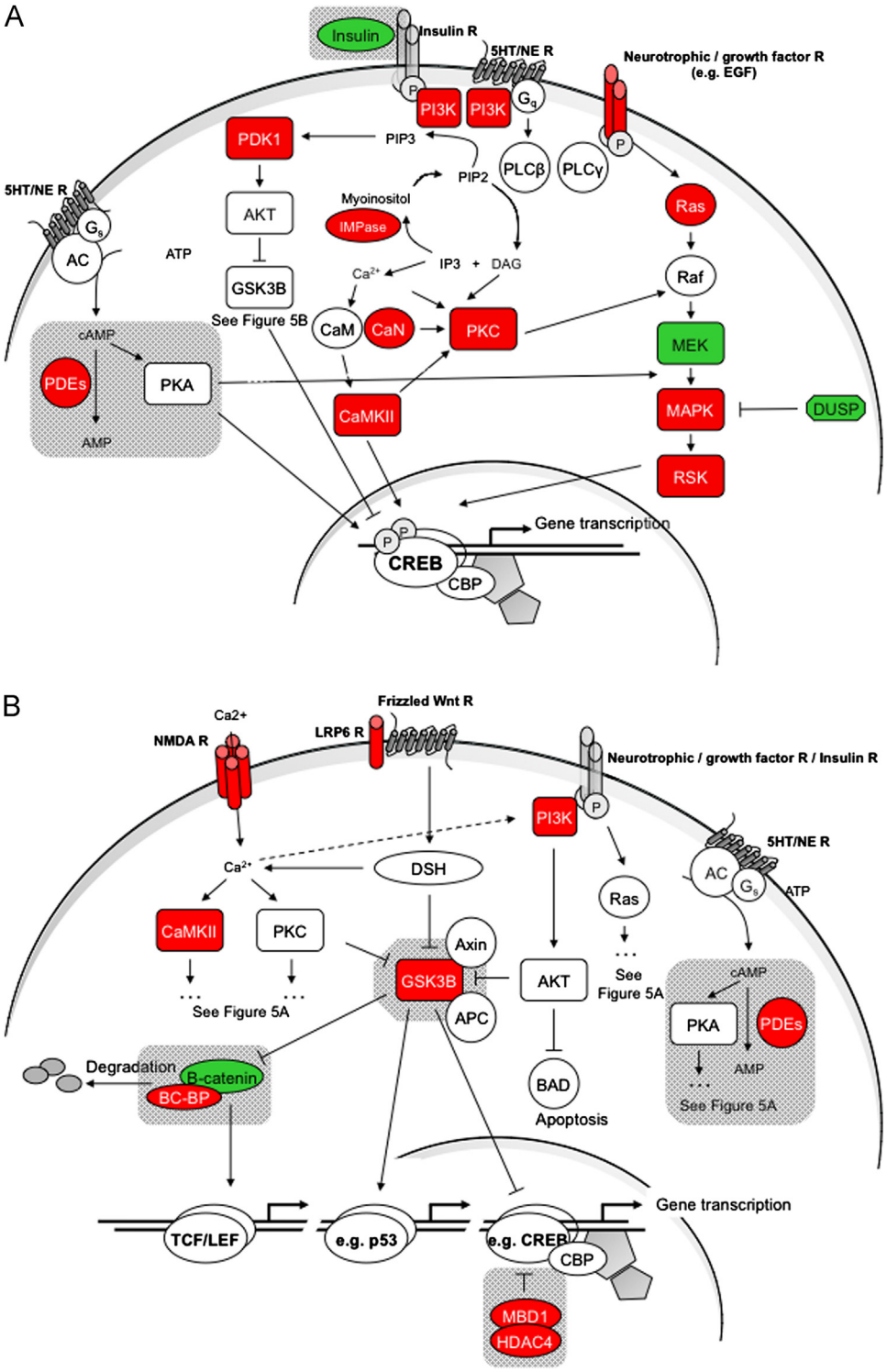

4.4. Limitations of the study

A major limitation of the present study is that the observed gene expression patterns may not be directly related to the behavioral measures assessed in the present study. For example, the observed changes in gene expression may just as well be associated with cognitive changes seen with PS (Zuena et al., 2008). In fact, many of the affected biological processes are known to be related to various types of affective and cognitive behavior and may therefore explain a general increased susceptibility to psychopathology observed in PS subjects. Furthermore, it is likely that the behavioral testing paradigms exerted an independent effect on central gene expression profiles. Although behavioral task exposure was identical for all groups, one cannot exclude that the animals' response to it was different among groups. Thus, behavioral testing may have left a permanent imprint on hippocampal and frontal gene expression patterns in a sex- and/or condition-dependent manner. Obviously, examining behavior and its underlying biological mechanisms in the same set of animals enables the possibility of linking both features in a more direct way. Moreover, evidently, the use of homogenates does not allow us to discriminate which specific anatomical subregions and/or populations of cells are affected.

4.5. Concluding remarks

In conclusion, the present study shows that prenatal maternal stress in Sprague-Dawley rats is associated with clearly increased anxiety- and depression-related behavior in adult male, but not female offspring. Male PS offspring further showed increased basal plasma corticosterone levels, whereas both PS males and females failed to show an adequate response to stress with lower stress-induced corticosterone levels as compared to controls. While the behavioral effects of PS were more pronounced in male offspring, gene expression was altered to a considerably greater extent in females. Thus, we hypothesize that part of the observed alterations in gene expression patterns in female offspring may indicate molecular mechanisms inducing resilience to PS. As such, microarray analysis within the hippocampus and FC highlighted various signaling pathways which may be critically involved in the development of mood disorders and/or the actions of antidepressants. Examples include glutamatergic and GABAergic signaling, the cAMP/cGMP/PDE system, the MAPK pathway, insulin signaling, and the GSK-3 signaling pathway. Altogether, the current study suggests that resilience to developmental stress exposure may be mediated, at least in part, via these intracellular signaling cascades. Furthermore, these signaling pathways may provide potential targets for novel antidepressant and mood stabilizing drug treatments, including e.g. HDAC inhibitors and PDE inhibitors.

Role of funding source

D.L.A. van den Hove, G. Kenis, K.P. Lesch, H.W.M. Steinbusch and J. Prickaerts were supported by the European Union Framework Integrated Project NEWMOOD Grant no. LSHM-CT-2004-503474. NEWMOOD had no further role in the study design; in the collection, analysis and interpretation of data; in the writing of the report; and in the decision to submit the paper for publication.

Contributors

Dr. Daniël L.A. van den Hove: Animal experiments, data analysis and writing;
Dr. Gunter Kenis: Microarray analysis, data analysis and writing, supervision of biochemical analysis;
Prof. Andrew Brass: Microarray analysis;
Rianne Opstelten: Overall data analysis, writing, proofreading and preparation of the manuscript;
Dr. Bart P.F. Rutten: General consultant;
Dr. Matteo Bruschettini: Animal experiments;
Prof. Carlos E. Blanco: Project coordinator, overall discussion and writing;
Prof. Klaus-Peter Lesch: General consultant;
Prof. Harry W.M. Steinbusch: Project coordinator, overall discussion and writing; and
Dr. Jos Prickaerts: Project coordinator, overall discussion and writing.

Figure 5 Schematic overview of signaling cascades affected by prenatal maternal stress within the female hippocampus (A) and frontal cortex (B). Genes upregulated by prenatal stress are highlighted in green (or light grey). Genes downregulated after prenatal stress are shown in red (or dark grey). Arrows represent positive interactions; T-shaped arrows indicate negative interactions. For more information, see text. Abbreviations: 5-HT/NE: Serotonin (5-HT)/ norepinephrine (NE); AC: Adenylate cyclase; AMP: Adenosine monophosphate; APC: Adenomatous polyposis coli; ATP: Adenosine triphosphate; BAD: BCL2-associated agonist of cell death; BC-BP: B-catenin binding protein; Ca^{2+}: Calcium $^{2+}$; CaM: Calmoduline; CaMKII: Ca^{2+}/calmodulin-dependent protein kinase; cAMP: Cyclic AMP; CaN: Calcineurin; CBP: CREB-binding protein; CREB: cAMP response element binding protein; DAG: Diacyl glycerol; DSH: Disheveled; DUSP: dual specificity phosphatase; EGF: Epidermal growth factor; G_q: Guanine-nucleotide binding protein, q; G_s: Guanine-nucleotide binding protein, stimulatory; GSK3B: Glycogen synthase kinase 3B; HDAC4: histone deacetylase 4; IMPase: Inositol monophosphatase; IP3: Inositol 1,4,5-triphosphate; MAPK: Mitogen-activated protein kinase; LRP6: Low-density lipoprotein receptor-related protein 6; MBD1: methyl-CpG-binding domain protein 1; MEK: MAPK kinase 1; NMDA: N-Methyl-D-aspartic acid; P: Phosphate/phospho-; p53: Protein 53; PDEs: Phosphodiesterases; PDK1: Phosphoinositide-dependent kinase 1; PI3K: Phosphoinositol 3-kinase; PIP2: Phosphatidylinositol (4,5)-bisphosphate; PIP3: Phosphatidylinositol (3,4,5)-trisphosphate; PKA: Protein kinase A; PKC: Protein kinase C; PLC: Phospholipase-C; R: Receptor; Raf: v-raf-1 murine leukemia viral oncogene; Ras: Rat sarcoma; RSK: Ribosomal protein S6 kinase; TCF/LEF: T-cell factor/lymphoid enhancer factor; Wnt: Wingless/Int. (For interpretation of the references to color in this figure legend, the reader is referred to the web version of this article.)

Conflict of interest

We hereby declare that there is no conflict of interest for any of the contributing authors of the present manuscript. Dr. G. Kenis has received financial compensation as an independent symposium speaker from Eli Lilly. Dr J. Prickaerts has received research funds from Johnson & Johnson PRD, Abbott, Intracellular Therapeutics and Envivo, which, however, were not related to the present work.

Acknowledgments

The authors would like to thank Dr. T. Hinsley (Department of Computer Science, University of Manchester, Manchester, M13 9PL, United Kingdom) for his contribution to the microarray analysis.

Appendix A. Supporting information

Supplementary data associated with this article can be found in the online version at http://dx.doi.org/10.1016/j.euroneuro.2012.09.011.

References

Aberg, N.D., Brywe, K.G., Isgaard, J., 2006. Aspects of growth hormone and insulin-like growth factor-I related to neuroprotection, regeneration, and functional plasticity in the adult brain. Sci. World J. 6, 53–80 PMID:16432628.

Alonso, S.J., Castellano, M.A., Quintero, M., Navarro, E., 1999. Action of antidepressant drugs on maternal stress-induced hypoactivity in female rats. Methods Find. Exp. Clin. Pharmacol. 21, 291–295.

Alttoa, A., Koiv, K., Hinsley, T.A., Brass, A., Harro, J., 2010. Differential gene expression in a rat model of depression based on persistent differences in exploratory activity. Eur. Neuropsychopharmacol. 20, 288–300.

Bale, T.L., 2011. Sex differences in prenatal epigenetic programming of stress pathways. Stress 14, 348–356.

Bender, A.T., Beavo, J.A., 2006. Cyclic nucleotide phosphodiesterases: molecular regulation to clinical use. Pharmacol. Rev. 58, 488–520.

Blehar, M.C., 1995. Gender differences in risk factors for mood and anxiety disorders: implications for clinical treatment research. Psychopharmacol. Bull. 31, 687–691.

Bolstad, B.M., Irizarry, R.A., Astrand, M., Speed, T.P., 2003. A comparison of normalization methods for high density oligonucleotide array data based on variance and bias. Bioinformatics 19 (2), 185–193 PMID: 12538238.

Bonow, R.H., Aid, S., Zhang, Y., Becker, K.G., Bosetti, F., 2009. The brain expression of genes involved in inflammatory response, the ribosome, and learning and memory is altered by centrally injected lipopolysaccharide in mice. Pharmacogenomics J. 9, 116–126.

Brown, E.S., Varghese, F.P., McEwen, B.S., 2004. Association of depression with medical illness: does cortisol play a role? Biol. Psychiatry 55, 1–9.

Chapman, R.H., Stern, J.M., 1978. Maternal stress and pituitary-adrenal manipulations during pregnancy in rats: effects on morphology and sexual behavior of male offspring. J. Comp. Physiol. Psychol. 92, 1074–1083.

Covington 3rd, H.E., Vialou, V.F., Laplant, Q., Ohnishi, Y.N., Nestler, E.J., 2011. Hippocampal-dependent antidepressant-like activity of histone deacetylase inhibition. Neurosci. Lett.

Daimon, M., Sato, H., Oizumi, T., Toriyama, S., Saito, T., Karasawa, S., Jimbu, Y., Wada, K., Kameda, W., Susa, S., Yamaguchi, H., Emi, T., Muramatsu, M., Kubota, I., Kawata, S., Kato, T., 2008. Association of the PIK3C2G gene polymorphisms with type 2 DM in a Japanese population. Biochem. Biophys. Res. Commun. 365 (3), 466–471. Epub 2007 November 6. PMID:17991425.

Dalla, C., Antoniou, K., Drossopoulou, G., Xagoraris, M., Kokras, N., Sfikakis, A., Papadopoulou-Daifoti, Z., 2005. Chronic mild stress impact: are females more vulnerable? Neuroscience 135, 703–714.

Darnaudery, M., Maccari, S., 2007. Epigenetic programming of the stress response in male and female rats by prenatal restraint stress. Brain Res. Rev..

De Kloet, E.R., Oitzl, M.S., 2003. Who cares for a stressed brain? The mother, the kid or both?. Neurobiol. Aging 24 (Suppl. 1), S61–S65 (discussion S67–S68).

Devaskar, S.U., Giddings, S.J., Rajakumar, P.A., Carnaghi, L.R., Menon, R.K., Zahm, D.S., 1994. Insulin gene expression and insulin synthesis in mammalian neuronal cells. J. Biol. Chem. 269, 8445–8454.

Dong, C., Wong, M.L., Licinio, J., 2009. Sequence variations of ABCB1, SLC6A2, SLC6A3, SLC6A4, CREB1, CRHR1 and NTRK2: association with major depression and antidepressant response in Mexican-Americans. Mol. Psychiatry 14, 1105–1118.

Dugovic, C., Maccari, S., Weibel, L., Turek, F.W., Van Reeth, O., 1999. High corticosterone levels in prenatally stressed rats predict persistent paradoxical sleep alterations. J. Neurosci. 19, 8656–8664.

Dunning, M.J., Smith, M.L., Ritchie, M.E., Tavaré, S., 2007. Beadarray: R classes and methods for Illumina bead-based data. Bioinformatics 23 (16), 2183–2184. Epub 2007 June 22. PMID: 17586828.

Duman, R.S., Monteggia, L.M., 2006. A neurotrophic model for stress-related mood disorders. Biol. Psychiatry 59, 1116–1127.

Emamian, E.S., Hall, D., Birnbaum, M.J., Karayiorgou, M., Gogos, J.A., 2004. Convergent evidence for impaired AKT1-GSK3beta signaling in schizophrenia. Nat. Genet. 36, 131–137.

Gould, T.D., Einat, H., Bhat, R., Manji, H.K., 2004a. AR-A014418, a selective GSK-3 inhibitor, produces antidepressant-like effects in the forced swim test. Int. J. Neuropsychopharmacol. 7, 387–390.

Gould, T.D., Zarate, C.A., Manji, H.K., 2004b. Glycogen synthase kinase-3: a target for novel bipolar disorder treatments. J. Clin. Psychiatry 65, 10–21.

Grayson, D.R., Kundakovic, M., Sharma, R.P., 2010. Is there a future for histone deacetylase inhibitors in the pharmacotherapy of psychiatric disorders? Mol. Pharmacol. 77, 126–135.

Grimes, C.A., Jope, R.S., 2001. The multifaceted roles of glycogen synthase kinase 3beta in cellular signaling. Prog. Neurobiol. 65, 391–426.

Gronli, J., Murison, R., Fiske, E., Bjorvatn, B., Sorensen, E., Portas, C.M., Ursin, R., 2005. Effects of chronic mild stress on sexual behavior, locomotor activity and consumption of sucrose and saccharine solutions. Physiol. Behav. 84, 571–577.

Halene, T.B., Siegel, S.J., 2007. PDE inhibitors in psychiatry – future options for dementia, depression and schizophrenia? Drug Disc. Today 12, 870–878.

Hashimoto, K., 2009a. Emerging role of glutamate in the pathophysiology of major depressive disorder. Brain Res. Rev. 61, 105–123.

Hashimoto, K., 2009b. Emerging role of glutamate in the pathophysiology of major depressive disorder. Brain Res. Rev. 61, 105–123.

Huang da, W., Sherman, B.T., Lempicki, R.A, 2009. Systematic and integrative analysis of large gene lists using DAVID bioinformatics resources. Nat. Protoc. 4, 44–57.

Huizink, A.C., Mulder, E.J., Buitelaar, J.K., 2004. Prenatal stress and risk for psychopathology: specific effects or induction of general susceptibility? Psychol. Bull. 130, 115–142.

Hur, E.M., Zhou, F.Q., 2010. GSK3 signalling in neural development. Nat. Rev. Neurosci. 11, 539–551.

Kaidanovich-Beilin, O., Milman, A., Weizman, A., Pick, C.G., Eldar-Finkelman, H., 2004. Rapid antidepressive-like activity of specific glycogen synthase kinase-3 inhibitor and its effect on beta-catenin in mouse hippocampus. Biol. Psychiatry 55, 781–784.

Kalueff, A.V., Nutt, D.J., 2007. Role of GABA in anxiety and depression. Depress. Anxiety 24, 495–517.

Kobayashi, M., Masaki, T., Hori, K., Masuo, Y., Miyamoto, M., Tsubokawa, H., Noguchi, H., Nomura, M., Takamatsu, K., 2005. Hippocalcin-deficient mice display a defect in cAMP response element-binding protein activation associated with impaired spatial and associative memory. Neuroscience 133, 471–484.

Krishnan, V., Nestler, E.J., 2008. The molecular neurobiology of depression. Nature 455, 894–902.

Laloux, C., Mairesse, J., Van Camp, G., Giovine, A., Branchi, I., Bouret, S., Morley-Fletcher, S., Bergonzelli, G., Malagodi, M., Gradini, R., Nicoletti, F., Darnaudery, M., Maccari, S., 2012. Anxiety-like behaviour and associated neurochemical and endocrinological alterations in male pups exposed to prenatal stress. Psychoneuroendocrinology.

Li, X., Jope, R.S., 2010. Is glycogen synthase kinase-3 a central modulator in mood regulation? Neuropsychopharmacology 35, 2143–2154.

Lustman, P.J., Clouse, R.E., 2005. Depression in diabetic patients: the relationship between mood and glycemic control. J. Diabetes Complications 19, 113–122.

Matrisciano, F., Tueting, P., Maccari, S., Nicoletti, F., Guidotti, A., 2012. Pharmacological activation of group-II metabotropic glutamate receptors corrects a schizophrenia-like phenotype induced by prenatal stress in mice. Neuropsychopharmacology 37 (4), 929–938 http://dx.doi.org/. 10.1038/npp.2011.274 Epub 2011 November 16. PMID:22089319.

McClung, C.A., Nestler, E.J., 2008. Neuroplasticity mediated by altered gene expression. Neuropsychopharmacology 33, 3–17.

McEwen, B.S., Magarinos, A.M., Reagan, L.P., 2002. Studies of hormone action in the hippocampal formation: possible relevance to depression and diabetes. J. Psychosom. Res. 53, 883–890.

Mill, J., Petronis, A., 2007. Molecular studies of major depressive disorder: the epigenetic perspective. Mol. Psychiatry 12, 799–814.

Morley-Fletcher, S., Darnaudery, M., Koehl, M., Casolini, P., Van Reeth, O., Maccari, S., 2003a. Prenatal stress in rats predicts immobility behavior in the forced swim test. Effects of a chronic treatment with tianeptine. Brain Res. 989, 246–251.

Morley-Fletcher, S., Rea, M., Maccari, S., Laviola, G., 2003b. Environmental enrichment during adolescence reverses the effects of prenatal stress on play behaviour and HPA axis reactivity in rats. Eur. J. Neurosci. 18, 3367–3374.

Morley-Fletcher, S., Darnaudery, M., Mocaer, E., Froger, N., Lanfumey, L., Laviola, G., Casolini, P., Zuena, A.R., Marzano, L., Hamon, M., Maccari, S., 2004. Chronic treatment with imipramine reverses immobility behaviour, hippocampal corticosteroid receptors and cortical 5-HT(1A) receptor mRNA in prenatally stressed rats. Neuropharmacology 47, 841–847.

Morley-Fletcher, S., Mairesse, J., Soumier, A., Banasr, M., Fagioli, F., Gabriel, C., Mocaer, E., Daszuta, A., McEwen, B., Nicoletti, F., Maccari, S., 2011. Chronic agomelatine treatment corrects behavioral, cellular, and biochemical abnormalities induced by prenatal stress in rats. Psychopharmacology (Berl) 217, 301–313.

Mueller, B.R., Bale, T.L., 2008. Sex-specific programming of offspring emotionality after stress early in pregnancy. J. Neurosci. 28, 9055–9065.

Noguchi, H., Kobayashi, M., Miwa, N., Takamatsu, K., 2007. Lack of hippocalcin causes impairment in Ras/extracellular signal-regulated kinase cascade via a Raf-mediated activation process. J. Neurosci. Res. 85, 837–844.

Ott, A., Stolk, R.P., van Harskamp, F., Pols, H.A., Hofman, A., Breteler, M.M., 1999. Diabetes mellitus and the risk of dementia: the Rotterdam study. Neurology 53, 1937–1942.

Owen, D., Matthews, S.G., 2003. Glucocorticoids and sex-dependent development of brain glucocorticoid and mineralocorticoid receptors. Endocrinology 144, 2775–2784.

Pilc, A., Chaki, S., Nowak, G., Witkin, J.M., 2008. Mood disorders: regulation by metabotropic glutamate receptors. Biochem. Pharmacol. 75, 997–1006.

Pittenger, C., Sanacora, G., Krystal, J.H., 2007. The NMDA receptor as a therapeutic target in major depressive disorder. CNS Neurol. Disord. Drug Targets 6, 101–115.

Poltyrev, T., Gorodetsky, E., Bejar, C., Schorer-Apelbaum, D., Weinstock, M., 2005. Effect of chronic treatment with ladostigil (TV-3326) on anxiogenic and depressive-like behaviour and on activity of the hypothalamic-pituitary-adrenal axis in male and female prenatally stressed rats. Psychopharmacology (Berl) 181, 118–125.

Poltyrev, T., Weinstock, M., 2004. Gender difference in the prevention of hyperanxiety in adult prenatally stressed rats by chronic treatment with amitriptyline. Psychopharmacology (Berl) 171, 270–276.

Porsolt, R.D., Anton, G., Blavet, N., Jalfre, M., 1978. Behavioural despair in rats: a new model sensitive to antidepressant treatments. Eur. J. Pharmacol. 47, 379–391.

Price, R.B., Shungu, D.C., Mao, X., Nestadt, P., Kelly, C., Collins, K.A., Murrough, J.W., Charney, D.S., Mathew, S.J., 2009. Amino acid neurotransmitters assessed by proton magnetic resonance spectroscopy: relationship to treatment resistance in major depressive disorder. Biol. Psychiatry 65, 792–800.

Prickaerts, J., Raaijmakers, W., Blokland, A., 1996. Effects of myocardial infarction and captopril therapy on anxiety-related behaviors in the rat. Physiol. Behav. 60, 43–50.

Reagan, L.P., 2007. Insulin signaling effects on memory and mood. Curr. Opin. Pharmacol. 7, 633–637.

Reneerkens, O.A., Rutten, K., Steinbusch, H.W., Blokland, A., Prickaerts, J., 2009. Selective phosphodiesterase inhibitors: a promising target for cognition enhancement. Psychopharmacology (Berl) 202, 419–443.

Renthal, W., Nestler, E.J., 2009. Chromatin regulation in drug addiction and depression. Dialogues Clin. Neurosci. 11, 257–268.

Robertson, S.D., Matthies, H.J., Owens, W.A., Sathananthan, V., Christianson, N.S., Kennedy, J.P., Lindsley, C.W., Daws, L.C., Galli, A., 2010. Insulin reveals Akt signaling as a novel regulator of norepinephrine transporter trafficking and norepinephrine homeostasis. J. Neurosci. 30, 11305–11316.

Salas, T.R., Reddy, S.A., Clifford, J.L., Davis, R.J., Kikuchi, A., Lippman, S.M., Menter, D.G., 2003. Alleviating the suppression of glycogen synthase kinase-3beta by Akt leads to the phosphorylation of cAMP-response element-binding protein and its transactivation in intact cell nuclei. J. Biol. Chem. 278, 41338–41346.

Sanguinetti, G., Lawrence, N.D., Rattray, M., 2006. Probabilistic inference of transcription factor concentrations and gene-specific regulatory activities. Bioinformatics 22 (22), 2775–2781. Epub 2006 September 11. PMID:16966362.

Schmidt, H.D., Duman, R.S., 2011. Peripheral BDNF produces antidepressant-like effects in cellular and behavioral models. Neuropsychopharmacology 35, 2378–2391.

Sheline, Y.I., Gado, M.H., Kraemer, H.C., 2003. Untreated depression and hippocampal volume loss. Am J. Psychiatry 160, 1516–1518.

Shepherd, J.K., Grewal, S.S., Fletcher, A., Bill, D.J., Dourish, C.T., 1994. Behavioural and pharmacological characterisation of the elevated ''zero-maze'' as an animal model of anxiety. Psychopharmacology (Berl) 116, 56–64.

Smirnov, A., Entelis, N., Martin, R.P., Tarassov, I., 2011. Biological significance of 5S rRNA import into human mitochondria: role of ribosomal protein MRP-L18. Genes Dev. 25 (12), 1289–1305. http://dx.doi.org/10.1101/gad.624711 PMID: 21685364.

Strackx, E., Van den Hove, D.L., Prickaerts, J., Zimmermann, L., Steinbusch, H.W., Blanco, C.E., Gavilanes, A.W., Vles, J.S.,

2009. Fetal asphyctic preconditioning protects against perinatal asphyxia-induced behavioral consequences in adulthood. Behav. Brain Res. 208, 343–351.

Sulon, J., Demey-Ponsart, L., Beauduin, P., Sodoyez, J.C., 1978. Radioimmunoassay of corticosterone, cortisol and cortisone: their application to human cord and maternal plasma. J. Steroid Biochem. 9, 671–676.

Tanis, K.Q., Duman, R.S., 2007. Intracellular signaling pathways pave roads to recovery for mood disorders. Ann. Med. 39, 531–544.

Tanis, K.Q., Newton, S.S., Duman, R.S., 2007. Targeting neurotrophic/growth factor expression and signaling for antidepressant drug development. CNS Neurol. Disord. Drug Targets 6, 151–160.

Taylor, W.D., Kuchibhatla, M., Payne, M.E., Macfall, J.R., Sheline, Y.I., Krishnan, K.R., Doraiswamy, P.M., 2008. Frontal white matter anisotropy and antidepressant remission in late-life depression. PLoS One 3, e3267.

Tsankova, N., Renthal, W., Kumar, A., Nestler, E.J., 2007. Epigenetic regulation in psychiatric disorders. Nat. Rev. Neurosci. 8, 355–367.

Van den Bergh, B.R.H., Mulder, E.J.H., Mennes, M., Glover, V., 2005. Antenatal maternal anxiety and stress and the neurobehavioural development of the fetus and child: links and possible mechanisms. A review. Neurosci. Biobehav. Rev. 29, 237–258.

Van den Hove, D.L., Blanco, C.E., Aendekerk, B., Desbonnet, L., Bruschettini, M., Steinbusch, H.P., Prickaerts, J., Steinbusch, H.W., 2005. Prenatal restraint stress and long-term affective consequences. Dev. Neurosci. 27, 313–320.

Van den Hove, D.L., Kenis, G., Steinbusch, H.W., Blanco, C.E., Prickaerts, J., 2010. Maternal stress-induced reduction in birth weight as a marker for adult affective state. Front Biosci. (Elite ed.) 2, 43–46.

Wada, A., 2009. Lithium and neuropsychiatric therapeutics: neuroplasticity via glycogen synthase kinase-3beta, beta-catenin, and neurotrophin cascades. J. Pharmacol. Sci. 110, 14–28.

Ward, I.L., Weisz, J., 1984. Differential effects of maternal stress on circulating levels of corticosterone, progesterone, and testosterone in male and female rat fetuses and their mothers. Endocrinology 114, 1635–1644.

Waterland, R.A., Jirtle, R.L., 2004. Early nutrition, epigenetic changes at transposons and imprinted genes, and enhanced susceptibility to adult chronic diseases. Nutrition 20, 63–68.

Weinstock, M., 2001. Alterations induced by gestational stress in brain morphology and behaviour of the offspring. Prog. Neurobiol. 65, 427–451.

Willner, P., Muscat, R., Papp, M., 1992. Chronic mild stress-induced anhedonia: a realistic animal model of depression. Neurosci. Biobehav. Rev. 16, 525–534.

Wong, M.L., Whelan, F., Deloukas, P., Whittaker, P., Delgado, M., Cantor, R.M., McCann, S.M., Licinio, J., 2006. Phosphodiesterase genes are associated with susceptibility to major depression and antidepressant treatment response. Proc. Natl. Acad. Sci. USA 103, 15124–15129.

Yang, P.C., Yang, C.H., Huang, C.C., Hsu, K.S., 2008. Phosphatidylinositol 3-kinase activation is required for stress protocol-induced modification of hippocampal synaptic plasticity. J. Biol. Chem. 283 (5), 2631–2643 Epub 2007 December 5. PMID:18057005.

Zhang, H.T., Huang, Y., Masood, A., Stolinski, L.R., Li, Y., Zhang, L., Dlaboga, D., Jin, S.L., Conti, M., O'Donnell, J.M., 2008. Anxiogenic-like behavioral phenotype of mice deficient in phosphodiesterase 4B (PDE4B). Neuropsychopharmacology 33, 1611–1623.

Zhang, L., Rubinow, D.R., Ma, W., Marks, J.M., Feldman, A.N., Barker, J.L., Tathan, T.A., 1998. GABA receptor subunit mRNA expression in brain of conflict, yoked control and control rats. Brain Res. Mol. Brain Res. 58, 16–26.

Zhao, W.Q., Alkon, D.L., 2001. Role of insulin and insulin receptor in learning and memory. Mol. Cell. Endocrinol. 177, 125–134.

Zuena, A.R., Mairesse, J., Casolini, P., Cinque, C., Alema, G.S., Morley-Fletcher, S., Chiodi, V., Spagnoli, L.G., Gradini, R., Catalani, A., Nicoletti, F., Maccari, S., 2008. Prenatal restraint stress generates two distinct behavioral and neurochemical profiles in male and female rats. PLoS One 3, e2170.